AD 661862

DISTRIBUTION OF THIS DOCUMENT IS UNLIMITED

HYDRONAUTICS, incorporated
research in hydrodynamics

Research, consulting, and advanced engineering in the fields of NAVAL and INDUSTRIAL HYDRODYNAMICS. Offices and Laboratory in the Washington, D. C., area: Pindell School Road, Howard County, Laurel, Md.

64

HYDRONAUTICS, Incorporated

TECHNICAL REPORT 605-1

EFFECTS OF AMBIENT CONDITIONS, THE GRAVITY FIELD, AND STRUTS, ON FLOWS OVER VENTILATED HYDROFOILS

By

R. Altmann and C. Elata

May 1967

DISTRIBUTION OF THIS DOCUMENT IS UNLIMITED

This Work was carried out under the
Naval Ship Systems Command
General Hydromechanics Research Program
Administered by the
Naval Ship Research and Development Center
Under
Contract N00014-66-C0003

BLANK PAGE

TABLE OF CONTENTS

LIST OF FIGURES

NOTATION

$C_{D_{cav}}$	Cavity drag coefficient of supercavitating hydrofoil section $C_{D_{cav}} = \frac{D_{cav}}{\frac{1}{2}\rho U_o^2}$
C_L	Lift coefficient $= \frac{L}{\frac{1}{2}\rho U_o^2}$
D_{cav}	Cavity drag of supercavitating hydrofoil, pounds
L	Lift, pounds
P_{cav}	Pressure within the hydrofoil cavity, pounds per square foot
P_v	Vapor pressure of water, pounds per square foot
P_o	Static pressure on undisturbed free streamline, pounds per square foot
U_o	Free stream velocity, feet per second
b	Foil span, feet
c	Foil chord, feet
d	Distance (general)
g	Gravitational acceleration constant = 32.196 fps^2
h	Submergence depth beneath free surface, feet
ℓ	Cavity length, feet
t	Cavity maximum thickness, feet

v	Downwash velocity, fps
x	Streamwise coordinate
y	Height (or depth) coordinate
z	Spanwise coordinate
α	Reference line angle of attack of hydrofoil
α_1	Induced angle of flow, measured from free stream
Γ	Net circulation
Δ	Representing a "change" in some function, such as $\Delta\alpha$, change in angle of attack
δ	Foil design angle of attack
κ	Tulin two-term camber index, effective value
κ_∞	Tulin two-term camber index for infinite depth of submergence operation
ξ	Representing chordwise position on a foil
ρ	Density of water, lb-sec^2/ft^4
σ_{cav}	Cavity cavitation number = $\dfrac{P_o - P_{cav}}{\frac{1}{2}\rho U_o^2}$
τ	Quasi-parabolic thickness index, effective

τ_∞	Parabolic thickness index for infinite depth of submergence operation
Ω_o	Maximum local value of circulation distributed over cavity
$\Omega(x)$	Local circulation distributed as a function of streamwise position over cavity

ABSTRACT

A series of experiments was conducted to determine the effects on foil performance of changes in cavity pressure and submergence depth. With fully-ventilated foils, drag and lift coefficients were found to be proportional to $(1 + \sigma_{cav})$, as predicted by theory. For base-ventilated foils a different and unexpected dependence of drag and lift on the cavity cavitation number was observed. Lift and drag on fully ventilated hydrofoils were also found to be almost unaffected by changes in submergence depth over the range of practical interest, as predicted by theory. However, the magnitudes of the measured forces were found to be smaller than predicted values. A simple analysis was made of the possible effect of the gravity field on foil performance. Further support for the idea that the gravity field may exert considerable influence was obtained through a series of tests in which ventilated hydrofoils were operated at both positive and negative angles of attack.

Measurements were also made to determine the effects of struts on ventilated hydrofoil cavity contours. Indirectly, these tests also assessed the magnitude of the strut-induced downwash. A considerable downwash was found to exist, having a profound effect on the cavity shape over the hydrofoil. Recent linearized theory on the magnitude of this strut-induced downwash correlates very well with the measurements.

INTRODUCTION

This is the second report of three on the experimental investigation of some basic properties of ventilated cavity flows. In the first report, (Reference 1), a study was made of cavity streamlines over two hydrofoils in essentially two-dimensional flow. Results of that experimental study showed that while existing theoretical treatment adequately describes the variations in cavity shape which occur with changes in submergence depth and angle of attack, theory does not accurately predict the heights of the cavity streamlines above the foil for any one given operating condition. Measured cavity ordinates are consistently less than predicted by theory.

In the present study a series of force measurements on the same hydrofoils was undertaken to examine the causes for this difference between theory and experiment. The description of these measurements and the conclusions drawn from them form the first part of this report.

An important conclusion of this part of the report is that forces on ventilated foils are substantially lower than predicted by theory. Therefore, for the second portion of this report, a simple analysis of the possible effects of the gravity field on the performance of ventilated hydrofoils was undertaken in an attempt to explain these differences, and a short series of tests was carried out to measure the effect of the gravity field. These tests appear to validate the premise that theories in which gravity effects are neglected may be inadequate to describe ventilated cavity flows.

The third part of this report describes a study of the effects of struts on the shape of cavities over hydrofoils. Cavity contours were observed in the proximity of three different struts. Measurements show a substantial decrease in hydrofoil cavity height near struts. The magnitude of this decrease is sufficient to render schemes of providing foil ventilating air through ports or notches at the sides of struts impractical, unless the foil is locally twisted to account for the downwash induced in the flow by the strut. To obtain some quantitative estimate of the magnitude of this downwash, an approximation to the strut-induced flow angles over the foil was obtained from the cavity contours. These angles, in turn, were compared to the linearized theory of strut-induced downwash, and favorable agreement between theory and experiment was observed.

Part One: Dependence of Force Coefficients on Flow Conditions

Recently, a number of experimental studies have been conducted in which the forces on three-dimensional hydrofoils were measured for varying angles of attack (References 2 to 6). The tests reported here were conducted to determine the effects of some lesser explored parameters on foil performance. Tests were planned to determine if existing theory can adequately describe changes in foil performance caused by changes in cavity cavitation number and changes in submergence depth, as well as by change in foil angle of attack. These tests were run with a thick, propeller-type, hydrofoil having considerable parabolic thickness and built-in angle of attack,as well as with a wedge hydrofoil, in order to ascertain the usefulness of the linearized theory in predicting the performance of very thick foil sections.

Previous work (Reference 1) had shown that cavity ordinates calculated from theory were consistently higher than those actually measured. It was felt to be of utmost importance to determine whether other parameters of foil performance are also different from those predicted by theory. Such correlated discrepancies in both cavity ordinates and foil forces might indicate an invalid fundamental assumption in the theoretical development. Hence, the measured, two-dimensional lift and drag coefficients of the tested hydrofoils were carefully compared to those predicted by theory.

Experimental Procedures

The two hydrofoil sections used for cavity streamline measurements, and described in Reference 1, were also used for the force measurements reported here. These hydrofoils were a wedge section of 16 percent thickness, and a thick, cambered section of $\tau_\infty = .05$, $\kappa_\infty = .0678$, and $\delta = 3$ degrees. A complete description of these section characteristics and their effects on foil performance is given in References 7 and 8; offsets of these sections are presented in Figure 1.

Both foils were of twenty inch span, and were supported at midspan by a 12 percent thick double ogive strut (see Figure 15). The ends of the foils were fastened to large, thin, tip plates, which served both to support the foils and to render the flow essentially two-dimensional over the foils and for a distance of two chords (six inches) downstream of the foil trailing edge.

All air used to ventilate the foil cavity was supplied through one of the tip plates, and by regulating air flow, cavity pressure could be varied. Cavity pressures were measured with a water manometer connected through tubing inside the double ogive strut to the trailing edge of the foil.

Forces on the hydrofoil, strut, and tip plates were measured by variable reluctance transducers mounted on the model support structure of the HYDRONAUTICS, Incorporated Variable-Pressure, Free-Surface, High-Speed Water Channel. A complete description of this facility, in which submergence depth, water speed, ambient pressure, and foil angle of attack can rapidly be varied, is given in Reference 9. The measured forces were displayed numerically on a digital readout system, and were recorded, along with all pertinent flow information, on IBM data cards.

To obtain the forces generated by the hydrofoil alone it was necessary to subtract from the total measured lifts and drags the contributions of the end plates and the double-ogive strut. A series of tests were therefore conducted in which forces on these bodies were measured separately. The lift produced by these supports was negligible. Their drag was found to be a function of submergence depth and angle of attack.

Since the two-dimensional section drag was of primary interest, the net hydrofoil drag had to be further reduced by removing the contributions of its frictional and induced drags. Frictional drag was estimated, using a coefficient of frictional resistance of .003.

Although the tip plates served to render flow over the foil nearly two-dimensional, and the downstream behavior of the cavity showed a lack of any trailing vortex "roll-up", some induced effects were nonetheless anticipated. Their contribution to foil drag was calculated, using the technique discussed in Reference 10, which is described in detail in Appendix B of this report.

Corrections for the wall effects of the channel were applied using the methods of Reference 3 as described in Appendix C.

The accuracies of all measurements were estimated and are presented in Appendix A.

Effect of Cavity Cavitation Number

In Figures 2 and 3 lift and drag data of the two sections are shown as functions of cavity cavitation number, σ_{cav}. The theory predicting the affect of σ_{cav} on foil performance is discussed in Reference 8. To the first order, both lift and drag on ventilated hydrofoils should increase by a factor of $(1 + \sigma_{cav})$. To obtain a value for the lift and drag of the two sections at $\sigma_{cav} = 0$ the best-fit straight lines through the data of Figures 2 and 3 were extrapolated. Theoretical lines, based on the $(1 + \sigma_{cav})$ correction factor, were drawn. These are the dashed lines of Figures 2 and 3.

Agreement between theory and experiment is very good for both foils when operating fully ventilated, and there is no need to refine the first order approximation derived in Reference 8 for the usual operating range of cavity cavitation number.

However, for conditions in which the hydrofoil operates base-vented, an unusual and unexpected behavior is noted. The cavity drag rises considerably faster than the $(1 + \sigma_{cav})$ factor, while lift is substantially reduced! Hitherto it had been intuitively assumed that the cavity drag of a base-vented foil would increase with $(1 + \sigma_{cav})$, while lift would remain unchanged. The data of Figures 2 and 3 show that this assumption is not valid.

The effect of cavity pressure on the behavior of base-vented foils has considerable practical importance. Base-vented sections appear to have a promising future for use in the transition speed ranges between those for which conventional airfoil and supercavitating hydrofoils are applicable. Moreover, even supercavitating hydrofoils will operate in the base-vented flow regime during certain conditions. If cavity pressure fluctuations are accompanied by surges in the foil lift and drag during these critical conditions, serious control problems might result. Further investigation of this phenomenon should definitely be undertaken.

Effect of Submergence Depth

The effect of changes in submergence depth on two-dimensional force coefficients was also examined during these tests. It is concluded in Reference 2 that the effects of submergence on the lift and drag of a three-dimensional hydrofoil are negligible. The linearized theory of supercavitating sections, presented in References 7 and 8, supports this conclusion by indicating that changes in section force coefficients with depth are very small over the practical operating range. A series of tests at various submergence depths was conducted on the thick, cambered foil to verify this prediction for the two-dimensional behavior.

The lift and drag coefficients for this section are plotted against submergence depth in Figures 4 and 5. In these same figures the predictions of linearized theory are shown since the hydrofoil was tested over a range of depths. An evaluation of the contributions of camber and parabolic thickness to lift and drag at off-design conditions was necessary. The techniques described in Reference 1 were utilized to obtain these corrections. To assess the contribution of angle of attack to lift and drag, Green's "exact" solution for the flow about a flat plate, as presented in Reference 6 has been utilized. This method was preferred to the linearized theory, since the angles of attack involved are relatively large.

It can be seen from Figures 4 and 5 that drag and lift coefficients are almost independent of submergence depth over most of the operating range, as predicted by theory. The values of the predicted coefficients differ from those obtained experimentally however, which will be discussed in the next section.

Part Two: The Effect of Gravity on Ventilated Cavity Flows

Differences in Theoretically Predicted and Measured Forces

It will be noted in Figures 4 and 5 that although the curves of the measured and theoretical force coefficients are almost parallel, there is a considerable difference between the absolute values of these coefficients at any one operating condition.

This difference appeared in all data obtained from the testing series. It is typified by the plots of Figures 6 and 7. Both the measured lifts and drags of each foil tested fall considerably below their theoretically calculated values; the difference appears equivalent to a shift in operating angle of attack on the order of three degrees.

It seems therefore, that an analogous situation does exist in theoretically predicted forces and cavity ordinates. In both cases the theory overestimates the results. It must be emphasized that this discrepancy cannot be considered merely a "non-linear" effect, caused by the practical limitations of applying linearized theory to foils of finite thickness. As has been outlined, non-linear corrections have been applied to the contribution of camber to lift, and the contribution of angle of attack was computed utilizing Greens "exact" solution, which is a non-linear solution to the flat plate lifting problem. Hence some hitherto unexamined phenomenon must be considered in order to explain the significant differences shown to exist between theory and experiment.

The Finite Froude Number Concept

An area of recent theoretical interest has been the effect of gravity fields on cavity flows. Both the linearized theory and Green's more exact solution assume the gravity effects to be very small when compared to the dynamic effects of the flow. If this assumption is not valid some deviation between theory and experiment must be expected.

Substantial information is available on various approaches to the problem of flow about a cavity in a gravity dominated field. The factors of forces, cavity pressures, cavity size and shape, induced flow angles, and free surface effects have, to various degrees, all been considered in these studies. References 11 to 14 are recommended as a historical introduction to this field. Unfortunately, existing theory cannot supply a direct answer to the complex, but practical, problem of the gravity field effect on flow about a ventilated hydrofoil of finite span, operating at some near-zero (but finite) cavity cavitation number, near the free surface. As a first step in understanding this practical problem the following analysis has been undertaken.

The assumption relegating negligible importance to the effects of gravity is synonymous to assuming an "infinite Froude number," which can be formulated as:

$$\frac{U_o}{\sqrt{g\ell}} \to \infty$$

where

U_o is the free stream velocity, fps

g is the gravitational acceleration constant, 32.196 fps^2, and

ℓ is the characteristic length, ft.

This condition may be approached when the free stream velocity becomes large or the characteristic length small. Essentially, very large Froude numbers imply that the static forces generated by any waves produced by the body, and the static buoyant forces acting on the body, are very small compared to the dynamic forces. Froude numbers based on a chord length of three inches and a velocity of twenty-five feet per second, (values typical of the foils examined here) are on the order of 10, a reasonably large number. However, for the study of ventilated cavity flows it is imperative to realize that the entire hydrofoil-cavity system influences the flow field, and that the cavity length, rather than the foil chord, is the characteristic length which must be considered. Froude numbers based on typical cavity lengths for the models tested for this report are only on the order of 2!

It therefore appears that significant gravity field effects may well be present in the tests described above, and the obvious next step is to estimate their magnitude.

Theoretical Considerations

To avoid complications in the early stages of analysis a very simple mathematical model of cavity flow will be used. The model, outlined in Figure 8, is two-dimensional; only buoyant forces on the cavity will be considered. The cavity, generated by a flat plate and springing from the flat plate trailing edge, is elliptic in its streamwise section. Major axis (length) is "ℓ", and minor axis(thickness) is "t".

Because it displaces a certain volume of water there will be a buoyant lift on the cavity equal to:

$$L = \rho_g \frac{\pi}{4} \ell t$$

where

ρ is the mass density of water.

Since the cavity is not accelerating upward but is in equilibrium beneath the free surface, some dynamic downward force must be exerted upon it by the fluid to just compensate the hydrostatic forces while maintaining a constant pressure on the cavity streamline. Such a force can only be generated by velocity perturbations in the fluid. Specifically, the lower surface of the cavity must have higher than free stream velocities near it, while the upper surface of the cavity must be surrounded by fluid with lower than free stream velocities.* Hence the concept of a circulation about the cavity to produce a net downward force can be qualitatively verified. Using the previously derived value for the buoyant lift on the cavity as the approximate total downward force this circulation must exert, the circulation may be determined to be

$$\Gamma = \frac{g\pi \ell t}{4U_o}$$

* A somewhat different visualization of this concept is to utilize the Bernoulli condition of constant total energy along any one streamline. Thus, the streamlines passing over the cavity must experience a decrease in kinetic energy (velocity) to balance their increase in potential energy (elevation). The opposite holds for those streamlines passing below the cavity.

Beyond this point a number of variations are possible, depending on the manner in which the circulation is distributed over the cavity. Figure 8 illustrates three approaches; two are extreme cases; one is a possibly realistic distribution.

The first and simplest variation is to allow the circulation to be concentrated at the center of the cavity. The downwash velocity any distance "d" from the cavity center then becomes

$$v = \frac{\Gamma}{2\pi d}$$

or, if the point of interest is on the flat plate and denoted as ξ

$$v(\xi) = \frac{g\ell t}{8U_o(\ell/2 + \xi)} \qquad [1]$$

An opposite extreme is to assume the circulation to be distributed uniformly over the cavity length. A local circulation must now be defined, equal to a constant value

$$\Omega(x) = \Omega_o,$$

such that

$$\Gamma = \int_o^\ell \Omega(x)\, dx.$$

For this case of a uniform distribution of circulation the above is solved such that

$$\Omega_o = \frac{gt\pi}{4U_o}$$

The downwash velocity at any point ξ is now the integrated effect of the downwash due to the circulation $\Omega(x)$ existing at all points x, or

$$v(\xi) = \int_o^{\ell} \frac{gt\pi}{4U_o(2\pi)(x+\xi)} \; dx \; .$$

This reduces to

$$v(\xi) = \frac{gt}{8U_o} \; \ell n \left|\frac{\ell+\xi}{\xi}\right| \; . \qquad [2]$$

It may be seen that as $\xi \rightarrow 0$, that is, as the cavity leading edge is approached, the downwash velocity becomes large without bound. This is due to the requirement of constant circulation at all points on the cavity.

A more realistic assumption is the specification of a parabolic circulation distribution over the cavity length. Choosing

$$\Omega(x) = \Omega_o \left[1 - \frac{4}{\ell^2} \left(x - \frac{\ell}{2}\right)^2\right]$$

a value of

$$\Omega_o = \frac{3\pi gt}{8U_o}$$

is obtained in the same manner as described in the second case above. The downwash at any point ξ then is given by

$$v(\xi) = \int_0^{\ell} \frac{\left(\frac{3\pi gt}{8U_o}\right)\left(1 - \frac{4}{\ell^2}\left[x - \frac{\ell}{2}\right]^2\right)}{2\pi(x+\xi)}\,dx,$$

which becomes after integration

$$v(\xi) = \frac{3gt}{4\ell U_o}\left\{\frac{\ell}{2} + \xi\left[1 + \left(1 + \frac{\xi}{\ell}\right)\ell n\left(\frac{\xi}{\xi+\ell}\right)\right]\right. \qquad [3]$$

The induced angles produced at ξ are simply the ratios of these downwash velocities to the free stream velocity U_o. Equations [1] and [3] may be considerably simplified by allowing $\ell \gg \xi$, a very realistic approximation. Using this approximation and solving the equations for the particular case of the three-quarter chord line ($\xi = c/4$), the resultant downwash angles due to the buoyancy of the cavity as calculated by the above methods compare as shown in Table 1.

TABLE 1

Downwash at Foil 3/4 Chord Due to Buoyant Cavity

Flow Conditions*	Assumed Circulation Distribution	α_1 (3/4 Chord)	α_1 (3/4 Chord)
$U_o = 25$ fps $t = .333$ ft	Concentrated at Center	$\frac{1}{4}\frac{gt}{U_o^2}$	$.24^\circ$
$c = .250$ ft $\ell = 4.00$ ft $h = .250$ ft	Constant over Cavity $\Omega(x) = \Omega_o = \frac{gt\pi}{4U_o}$	$\frac{1}{8}\ln\left(4\frac{\ell}{c}+1\right)\frac{gt}{U_o^2}$	$.51^\circ$
$\alpha = 8\frac{1}{2}^\circ$	Parabolic over Cavity $\Omega(x) = \Omega_o\left[1 - \frac{4}{\ell^2}\left(x - \frac{\ell}{2}\right)^2\right]$ $\Omega_o = \frac{3\pi gt}{8U_o}$	$\frac{3}{8}\frac{gt}{U_o^2}$	$.36^\circ$

* Input for column 1 was obtained from data to be discussed in the next section.

A further important concept can be derived from this form of analysis. Consider the model in which the circulation is assumed concentrated at the center of the cavity. Then,

$$\alpha_i = \frac{1}{4} \frac{t}{c} \frac{gc}{U_o^2} .$$

Two relations for ventilated cavities are now employed to rewrite this equation. First, for cavities open to the atmosphere, the cavitation number based on cavity pressure is

$$\sigma_{cav} = 2 \frac{h}{c} \frac{gc}{U_o^2} .$$

Secondly, from linearized theory for cavity flows at deep depths, (Reference 17),

$$\frac{t}{c} = \frac{2C_{D_o}}{\pi\sigma_{cav}} ,$$

where C_{D_o} refers to the drag coefficient at zero cavity cavitation number.

Using these relations, the induced angle due to the gravity may be expressed as

$$\alpha_i = \frac{1}{4\pi} \frac{C_{D_o}}{\left(\frac{h}{c}\right)} .$$

That is, the induced angle due to gravity field influences, at least at deep depths of submergence, is not a function of the Froude number, (i.e., not a function of speed or gravity field strength, if $g > 0$), but rather only a function of drag and submergence depth! Whether the theoretical magnitude of gravity induced downwash remains independent of Froude number at shallow depths, is not now known. This remarkable conclusion (a downwash induced by the influence of gravity, but independent of Froude number) is in agreement with most existing force data obtained on supercavitating hydrofoils. In fact, the existence of such speed independent data has generally led to the erroneous conclusion that the neglect of gravity in theoretical treatments is indeed justified. Although this result is not rigorously proven, since it depends on a combination of relations derived for both finite and infinite depth flows, it indicates a possible explanation for differences that exist between current theory and experiment, while still upholding the experimentally observed fact that in general the force coefficients of ventilated foils are nearly independent of velocity.

The magnitude of this gravity induced downwash, as calculated by the previously discussed methods and presented in Table 1, is certainly not large enough to account for the large differences between theory and experiment shown in Figures 6 and 7. Of course, as depth decreases the tabulated values of the induced angle will increase considerably, since cavity length and thickness increase almost twofold as depth of submergence changes from one to one-quarter chords. In addition, certain effects should now be mentioned which heretofore have been ignored.

The above analysis does not account for a free surface image. This image circulation system, based on the requirement of constant free surface pressure, will serve to increase the downwash angles tabulated above, to the point of doubling them at the hypothetical condition of zero operating depth. No rigorous evaluation of this effect has been made at the present time.

Neither does the preceding analysis account for three-dimensional effects on the downwash. These will probably serve to reduce the gravity field effects, but no estimation can presently be given of their quantitative effect.

Finally, it must be remembered that the assumptions on which this analysis was based were chosen for ease in calculation rather than accuracy in representing the physical phenomenon involved. What is apparent from the preceding calculations is only that a measurable effect on the flow does exist due to the presence of large cavities. This effect may explain the differences between the measured and theoretical force coefficients observed in the tests conducted for this report, and the similar difference between theory and experiment recorded in the cavity contour measurements of Reference 1.

Experimental Observations

Ivanov, Reference 12, was possibly the first to suggest that differences between the measured force coefficients of two identical foils could be due to their alignment with the gravity field. Inasmuch as the gravity effect always produces a downwash in the flow, a section operating at negative angles of attack should generate more negative lift than theory indicates, just as a section operating at positive angles produces less positive lift than predicted. Using this approach it should be possible to indirectly measure the gravity-induced downwash by recording the forces on a foil run in both a normal orientation, and also with a sufficiently negative angle of attack to produce a cavity beneath itself. Data from the first series of tests could be compared to the linearized theory developed in Reference 9. For the second set of tests it would be necessary to use theory for a supercavitating foil operating above a free surface. Linearized theory describing this condition has been developed by Auslaender in connection with the cascade effect on supercavitating propellers, and is outlined in Reference 15.

A series of tests was run on the wedge hydrofoil, supported by only the large end plates and operating at various depths, speeds, and both positive and negative angles of attack. Air was artificially fed to the cavity through the end plates, and cavity pressure was controlled to maintain a constant, near zero, cavity cavitation number at all times. Only lift forces were measured. Data were reduced by the same process described earlier. It was not intended that the results of these tests would provide definitive answers to the problems of gravity induced downwash. Rather, they would indicate the magnitudes and trends of this effect and aid in planning further research on this phenomenon.

Typical data are shown in Figures 9 and 10 for the one-half chord submergence depth; data at other depths were similar. Of major importance is the fact that for this particular wedge foil, lift coefficients clearly exhibit a slight dependence on velocity, even though the cavity cavitation number is nearly constant! This definitely indicates some presently unaccounted for velocity effect on flow conditions.

For the case of the cavity above the foil, (Figure 9), the relation between velocity and downwash effect is not monotonic. Lift coefficients measured at 15 fps lie between those measured at 20 fps and 25 fps. The preceding theoretical analysis shows the downwash to be a function of not only free stream velocity but also of cavity thickness, and this may influence the above mentioned effect. For reference, the measured maximum cavity thickness in inches is recorded at each data point, but no attempt to correlate the results with cavity thickness has been made.

When operating with the cavity beneath the foil, (Figure 10), much shorter and thinner cavities are obtained for the same speed, depth, cavity pressure, and angle of attack than when in the usual operating condition. Hence the magnitude of the gravity induced downwash should be considerably less than that experienced with the cavity above the foil. Again, no attempt has been made to account for this factor in the data. The observed variation in cavity size with speed was not as severe as with the cavity above the foil, and the magnitude of the downwash was found to be monotonic with speed.

For comparison, both Figures 9 and 10 have been plotted together on a reduced scale in Figure 11. It is obvious that the large shift in angle of attack previously noted in the force data for foils at positive angles of attack also exists at negative angles and is at some speeds, of the same order of magnitude. Even though the previous theoretical development predicted gravity induced angles of the order of one degree, it appears from these data that the actual magnitude of the gravity induced downwash may be considerably greater.

Conclusions on the Gravity Field Effect

From the preceding it may be concluded that there is an induced downwash due to the gravity field, which is very significant for the case of high aspect ratio wings. It is obvious that our knowledge of this effect is limited, and presently insufficient to permit accurate quantitative predictions.

Future work on this effect should be undertaken. Such work should include a rigorous theoretical formulation of the gravity-influenced flow field beneath a free surface in the presence of a cavity. Realistic mathematical models will be needed, and expressions for the cavity dimensions as functions of depth, cavity pressure, Froude number, and the nature of the cavity generating body, will be required. (It should be noted that this last problem has not yet been fully solved). Three-dimensional influences will have to be incorporated if the analysis is to be usable in practice.

Simultaneously, a comprehensive experimental study of the effects of this downwash on two and three-dimensional supercavitating foil performance should be conducted, possibly using an approach such as was used in this preliminary study.

The solution to this problem may well be the most important task of present research into supercavitating flow phenomena. It is possible that it can explain the inability of supercavitating hydrofoils to achieve design lift coefficients and efficiencies (Reference 2), as well as the inability to maintain a ventilated cavity down to the design angle of attack (References 1 and 3).

Part Three: The Effect of Struts on Cavity Contours Above Ventilated Hydrofoils

Interest in the problem of the effects of struts on foil performance was aroused when cavitation was observed in way of struts on the pressure face of foils operating at positive angles of attack. A theoretical analysis of the downwash produced by struts was conducted by Huang, (Reference 16) Huang's calculations predict surprisingly high downwash angles near the struts; values as high as four degrees downwash for a 15 percent thick parabolic strut were predicted; similar results exist for wedge struts. The theoretical flow about fully wetted struts was found to be characterized by a downwash over the forward half of the strut and an upwash in way of the trailing edge.

If these results are accurate in both magnitude and direction, a considerable change in the local angle of attack of the hydrofoil panel will be necessary to prevent the foil cavity from "washing off" near the strut. Tests to substantiate Huang's predictions were conducted by measuring the contours of the ventilated cavity over a strut-supported hydrofoil at a series of spanwise locations near the strut. The apparatus and procedure used to obtain the profiles of a ventilated cavity formed over a hydrofoil beneath the free surface are given in Reference 1. An identical process was used to measure cavity contours in the second set of tests reported here. To determine the cavity ordinates at the strut itself, a grid was marked on the strut walls. Figure 12 shows the probe, used to measure the cavity dimensions.

The hydrofoil was the thick, cambered section of $\delta = 3^{\circ}$, $\kappa_{\infty} = .0678$ and $\tau_{\infty} = .05$ throughout the tests, a submergence depth of one chord and a reference line angle of attack of 3.74° to the undisturbed flow, were maintained.

Three struts, were used in this study. Their sections were parabolic, double ogive, and wedge shaped. Each had a maximum thickness of twelve percent of the chord. Details of these sections are given in Figure 13.

Figures 14, 15, and 16 show the measured contours of the cavity at various spanwise locations using the parabolic, double ogive, and wedge strut respectively. Contours labeled "At Strut" were obtained from the grid on the strut by visual observation. The latter curves end a considerable distance from the foil leading edge, since at the strut the downwash is too severe to permit the cavity to extend to the foil leading edge. In tests conducted with the ogive strut a severe crossflow over the foil downstream of the midchord region, caused deflections of the thin measuring probe. Near the strut these deflections were too large to permit accurate measurements of the cavity ordinates. Hence an extrapolation of data was necessary in this region, shown as the dashed line in Figure 15.

In Figures 17, 18 and 19 the same data were replotted to show cavity height versus spanwise distance from the strut at four chordwise positions. Dimensions are normalized with respect to the strut chord, which here is also equal to the foil chord. At a distance of one strut chord from the strut centerline the cavity ordinates are essentially equal to those of the bare foil as reported in Reference 1. As the strut is approached its downwash decreases the cavity ordinates until, at the strut wall, a minimum ordinate is reached. For the double ogive strut, the upwash generated over its downstream half increases the cavity height at the foil trailing edge as the strut is approached, until the very low velocities associated with the strut boundary layer cause a rapid decrease in cavity ordinate near the strut wall.

Also plotted in Figures 17, 18, and 19 are the local changes in angle of attack required to produce the measured variations in cavity ordinate. The change in cavity height as a function of angle of attack for this foil was obtained from the data presented in Reference 1. This approach is not rigorous, since it assumes that a local decrease in cavity ordinate is due to the local downwash velocity at the point of interest only. In reality, an integration of the downwash velocities over the entire foil would have to be performed to obtain an accurate representation of any one local downwash angle. However, for the parabolic and wedge struts the simplified approach has some quantitative value, since the downwash angles are relatively constant over the foil chord at any one spanwise location.

For the parabolic and wedge struts, the linearized theoretical predictions of strut induced downwash angles as determined by Huang, Reference 16, are also plotted in Figures 17 and 19. The curves of predicted downwash angles correspond well with the values obtained in the manner discussed above.

A comparison of cavity ordinates at the strut wall is made in Figure 20. The extent of wetted upper foil surface due to strut induced downwash appears to be a function of the entrance angle of the strut leading edge. The wedge strut, which has an included angle of 6.88°, causes the cavity to spring from the upper foil surface at ten percent of the chord at the foil leading edge. For the larger leading edge angle of the double ogive strut, this point shifts back to eighteen percent of the chord; on the parabolic strut, with its blunt leading edge, the cavity originates twenty-three percent of the chord from the leading edge.

The nearly identical trailing edge cavity ordinates of the parabolic and wedge struts indicate that, past the mid-chord region of base-vented struts, the maximum thickness of the strut has a greater effect on the downwash velocities than the slope of the strut walls.

It is concluded in Reference 16 that strut downwash has a negligible effect on the lift forces generated by foils of reasonably high aspect ratio. From the preceding data it can be concluded however, that the effect on cavity shape is very significant, and this has important bearing on practical foil design. If foil ventilation is to be accomplished by feeding air to the hydrofoil leading edge through ports in the side of the strut, notches along the side of the strut, or ports in the foil leading edge near the strut, it is imperative that the local foil angle of attack be increased to compensate for the downwash induced by the strut. If this is not done, separation will not occur over the foil upper surface in the region of the air supply, and ventilation will not be sustained at the design angle of attack.

CONCLUSIONS

1. The variation of lift and drag coefficients with cavity pressure, for fully ventilated foils, is adequately described by theory. Lift and drag are proportional to $1 + \sigma_{cav}$.

2. For base vented foils, drag forces are larger than those predicted by theory, while lift forces decrease, when the cavity cavitation number increases.

3. The change in force coefficients with submergence depth is very closely predicted by present theory.

4. The magnitude of the forces on a ventilated foil are lower than predicted by theory. This may be at least partially accounted for by the effects of gravity induced downwash.

5. On ventilated foils, in the vicinity of the strut, the downwash is substantial, verifying Huang's theoretical analysis. In order to achieve fully ventilated foils near the strut attachment, the local angle of attack has to be increased.

APPENDIX A

ESTIMATED ACCURACIES OF EXPERIMENTAL MEASUREMENTS

Measurement	Accuracy
Flow velocity	±.10 fps
Angle of attack	±.05 degrees
Submergence depth	±.05 inch
Lift force	±.30 lbs
Drag force	±.30 lbs
Air flow rate	±.60 cfm, at STP
Channel atmospheric pressure	±.10 ft Hg
Cavity pressure, $\sigma_{cav} > .03$	±.50 inch H_2O
Cavity pressure, $\sigma_{cav} < .03$	±.1 inch H_2O
Cavity length	±2.0 inches
Cavity Maximum thickness	±.25 inch
Streamwise position along cavity	±.020 inch
Spanwise position on cavity	±.020 inch
Vertical ordinate of upper cavity surface	±.004 inch

APPENDIX B

INDUCED DOWNWASH ANGLES FOR FOILS WITH LARGE TIP PLATES

A finite span foil with sufficiently large end plates will have an insignificantly small induced downwash when placed in an infinite extended fluid. Close to a free surface however an image system is created that induces a downwash which increases inversely with h/b. Thus a high span foil, even with tip plates, will have a significant induced downwash when operating near the free surface.

To estimate this effect the method outlined in [10] was used. The governing equation being

$$\alpha_i = \frac{K_a K_e C_L (1 + P)}{\pi A}$$

where

α_i = induced downwash angle of flow,

C_L = Lift coefficient (measured),

P = Planform correction factor (from Glauert as replotted in [18],

A = Foil aspect ratio,

K_a = Biplane correction factor adapted to hydrofoils, (from Durand as replotted in [18]),

K_e = $1/(1 + 2\ h_e/b)$, where

h_e = Submergence of end plates, here equal to foil submergence depth plus three inches, and

b = Foil span.

APPENDIX C

EFFECTS OF CHANNEL WALLS ON FLOWS OVER VENTILATED HYDROFOILS

Channel corrections, to account for the influence of the walls and bottom on the force data obtained during these tests, were made in three stages. First, a blockage correction was applied to account for the side walls of the channel restricting the flow about the hydrofoil. Secondly, a correction was made to remove the influence of the vortex image system in the side walls of the channel. Finally, a blockage correction based on the proximity of the bottom of the channel was applied. A correction for the vortex image system within the channel bottom was considered, but was found to be very slight in comparison to the influence of the side wall vortex image, and hence was not included.

The side wall blockage correction to the force data is treated in the same manner as wind tunnel blockage corrections, as derived in Reference 18, and is based on the concept that the primary effects caused by the restriced flow about the model may be determined by computing the influence of images of the model thickness distribution, represented as a source and sink system, in the channel walls. The resulting increase in the dynamic pressure of the flow requires the measured lift and drag coefficients to be reduced slightly.

Accompanying the thickness image in the channel side walls are images generated by the vortex system of the hydrofoil. The image vortex system serves to induce an upwash in the flow, which in turn has the effect of making the estimated free stream values of induced angle of attack and induced drag too small. The correction procedure, again taken from Reference 18, computes factors to account both for changes in induced flow angle and streamline curvature.

The final boundary correction to the data accounted for the near-bottom effects. Analysis (in Reference 18) indicates that the vortex image in the channel bottom has very slight influence compared to the side wall images, and can be neglected. Hence, the bottom effect is fundamentally a blockage correction, and is treated using the theory of Reference 19, modified as described in Reference 3. The correction procedure computes the induced flow angle as a function of cavity drag and proximity to the bottom. Since the cavity drag is found by subtracting induced and frictional drags from the total foil drag, and since the total induced drag is a function of the bottom correction, the process is necessarily iterative.

Reviewing the effects of the three correction processes, it is seen that flow velocity has been increased, thus decreasing the measured values of lift and cavity drag coefficients. However, the wall image correction and the bottom correction serve to increase the cavity drag coefficient, as well as increasing the effective angle of attack of the foil. The net effects of the correction are illustrated in Figure 21.

REFERENCES

1. Altmann, R. J., "Measurement of Cavity Shapes Above Ventilated Hydrofoils," HYDRONAUTICS, Incorporated Technical Report 457-1, November, 1965.

2. Dobay, G. F., "Performance Characteristics of the BuShips Parent Hydrofoil," David Taylor Model Basin Report 2084, August 1965.

3. Scherer, J. O., and Auslaender, J., "Experimental Investigation of the 5-Inch Chord Model of the BuShips Parent Supercavitating Hydrofoil," HYDRONAUTICS, Incorporated Technical Report 343-1, March 1964.

4. Scherer, J. O., and Auslaender, J., "Experimental Investigation of a Supercavitating Hydrofoil with Upper Surface Spoiler Flaps," HYDRONAUTICS, Incorporated Technical Report 343-2, December 1964.

5. Scherer, J. O., and Auslaender, J., "Experimental Investigation of a Supercavitating Hydrofoil with Trailing Edge Flaps," HYDRONAUTICS, Incorporated Technical Report 343-3, September, 1965.

6. Johnson, V. E., Jr., "Theoretical and Experimental Investigation of Supercavitating Hydrofoils Operating Near the Free Water Surface," NASA Technical Report R-93, 1961.

7. Auslaender, J., "The Linearized Theory for Supercavitating Hydrofoils Operating at High Speeds Near a Free Surface," Journal of Ship Research, Volume 2, October 1962.

8. Auslaender, J., "Low Drag Supercavitating Hydrofoil Sections," HYDRONAUTICS, Incorporated Technical Report 001-7, April 1962.

9. Johnson, V. E., Jr, and Goodman, A., "The HYDRONAUTICS Variable-Pressure, Free-Surface, High-Speed Channel," ASME Symposium on Cavitation Research Facilities and Techniques, May 1964.

10. Martin, M., "The Stability Derivatives of a Hydrofoil Boat," HYDRONAUTICS, Incorporated Technical Report 001-10 (I and II), January 1963.

11. Parkin, B. R., "A Note on the Cavity Flow Past a Hydrofoil in a Liquid with Gravity," California Institute of Technology Report 47-9, December 1957.

12. Ivanov, A. I., "On the Effect of Gravity Forces on the Hydrodynamic Characteristics of Foil Sections," Susostroeniye, No. 2, 1961.

13. Street, R. L., "A Note on Gravity Effects in Supercavitating Flows," Stanford University Department of Civil Engineering Technical Report 32, March 1964.

14. Tulin, M. P., "The Shape of Cavities in Supercavitating Flows," for Presentation at the International Congress for Theoretical and Applied Mechanics, Munich, September 1964.

15. Tulin, M. P., "Supercavitating Propellers," for Presentation at the Fourth ONR Symposium on Naval Hydrodynamics, 1962.

16. Huang, T. T., "Strut Induced Downwash," HYDRONAUTICS, Incorporated Technical Report 463-7, September 1965.

17. Tulin, M. P., "Supercavitating Flow Past Foils and Struts," for Presentation at the Symposium on Cavitation in Hydrodynamics, National Physical Laboratory, Teddington, England, September, 1955.

18. Pope, Alan, "Wind-Tunnel Testing," John Wiley and Sons, Inc., New York, 1954.

19. Ho, H. T., "Linearized Theory for a Supercavitating Hydrofoil Operating in a Fluid of Finite Depth," HYDRONAUTICS, Incorporated Technical Report 119-7, June 1963.

FOIL NO. 1

TABLE OF OFFSETS		
x	y_t	y_b
0.0	0.0	0.0
0.060	0.030	0.023
0.120	0.045	0.033
0.180	0.057	0.042
0.240	0.067	0.049
0.300	0.076	0.056
0.600	0.112	0.084
0.900	0.141	0.110
1.200	0.166	0.135
1.500	0.189	0.162
1.800	0.209	0.190
2.100	0.228	0.220
2.400	0.246	0.252
2.700	0.263	0.287
3.000	0.279	0.324

DESIGN ANGLE OF ATTACK δ 3.00°
TULIN TWO-TERM CHAMBER κ_∞ 0.0678
PARABOLIC THICKNESS τ_∞ 0.05

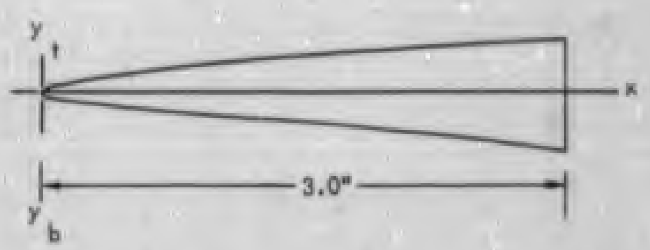

FOIL NO. 2

16% WEDGE

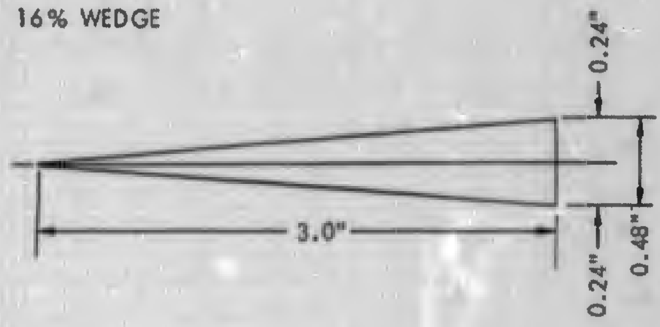

FIGURE 1 - OFFSETS OF FOIL SECTIONS TESTED

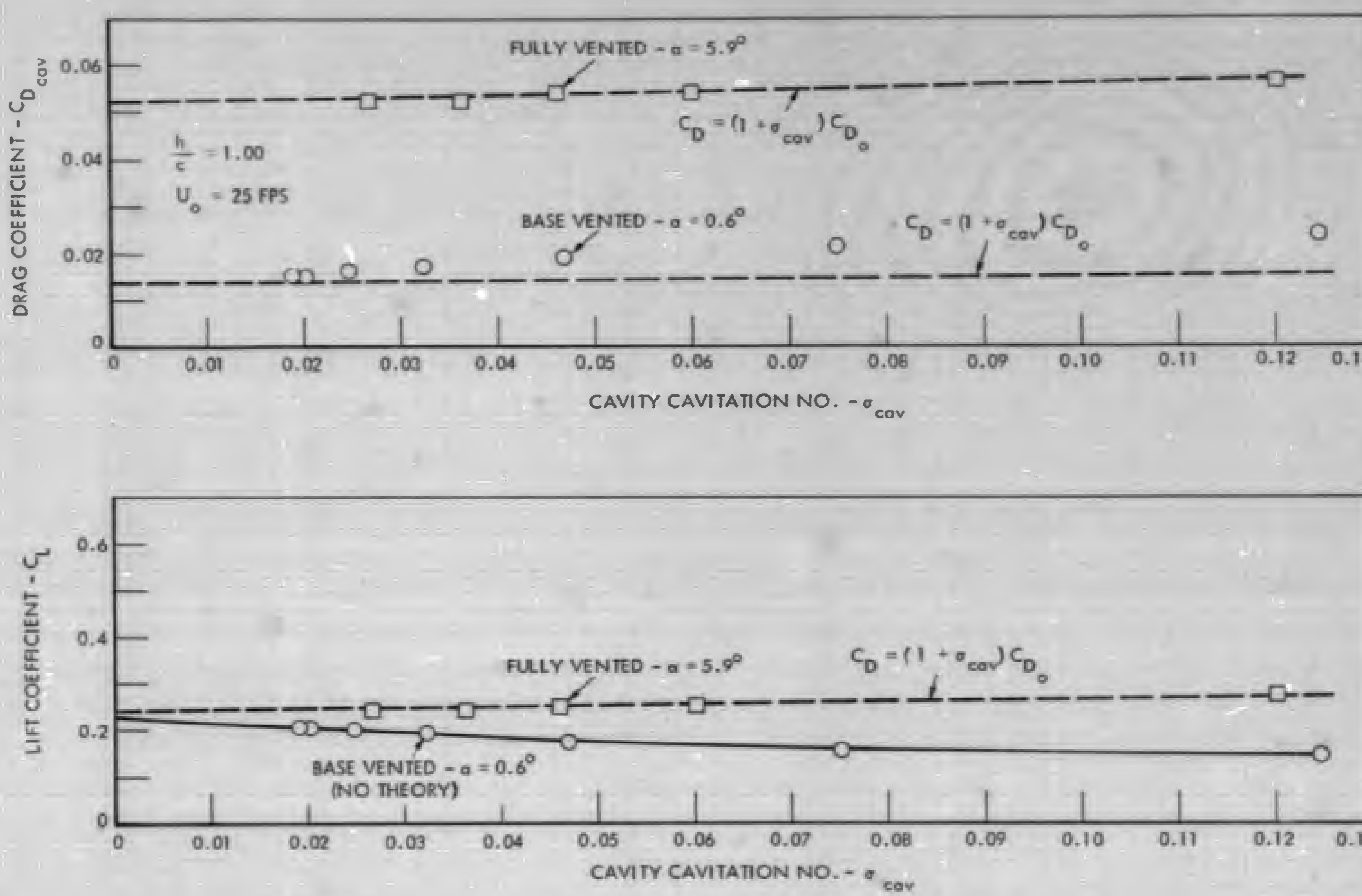

FIGURE 2 - FORCE COEFFICIENTS VERSUS CAVITY PRESSURE FOR THICK, CAMBERED SECTION

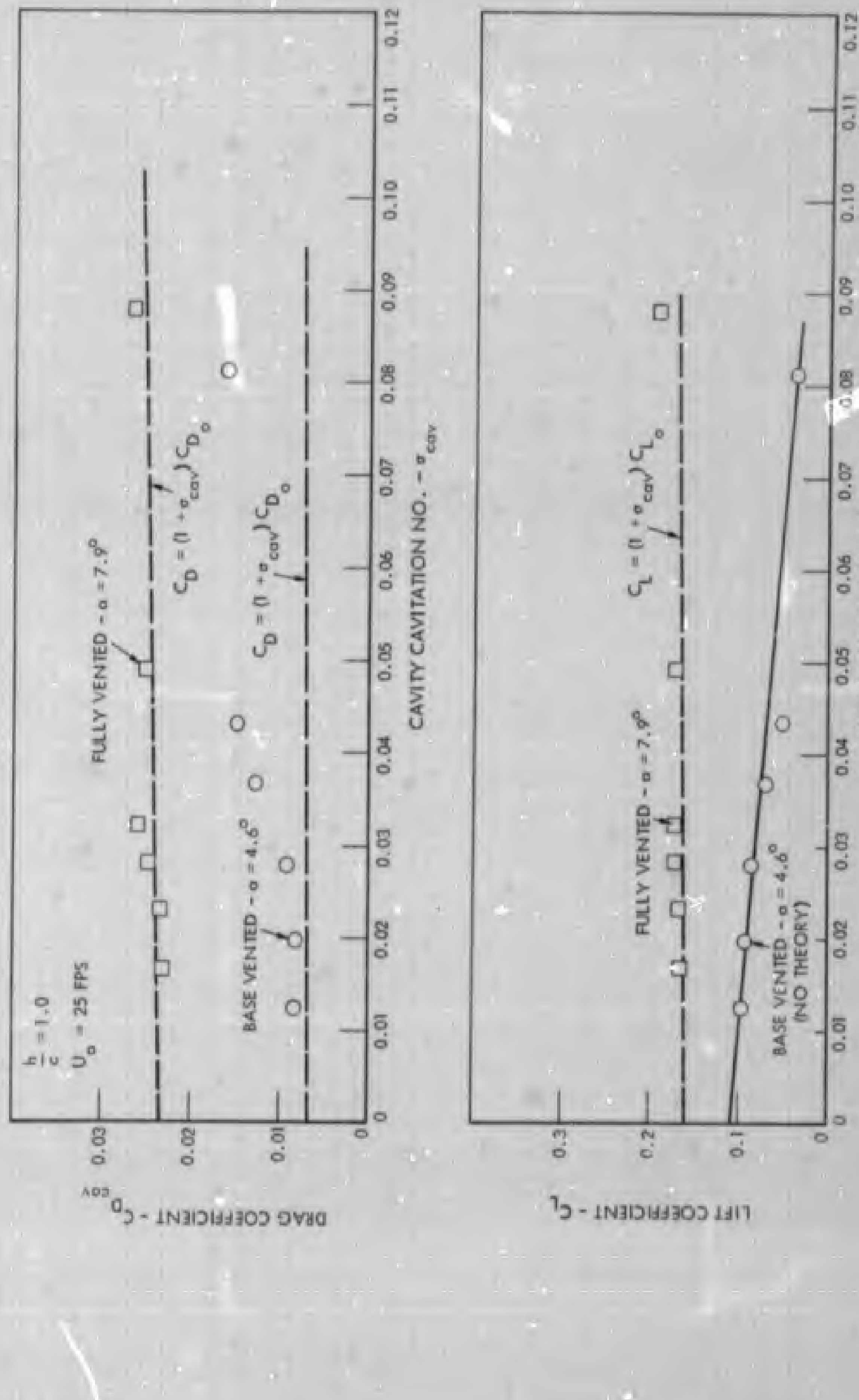

FIGURE 3 - FORCE COEFFICIENTS VERSUS CAVITY PRESSURE FOR WEDGE SECTION

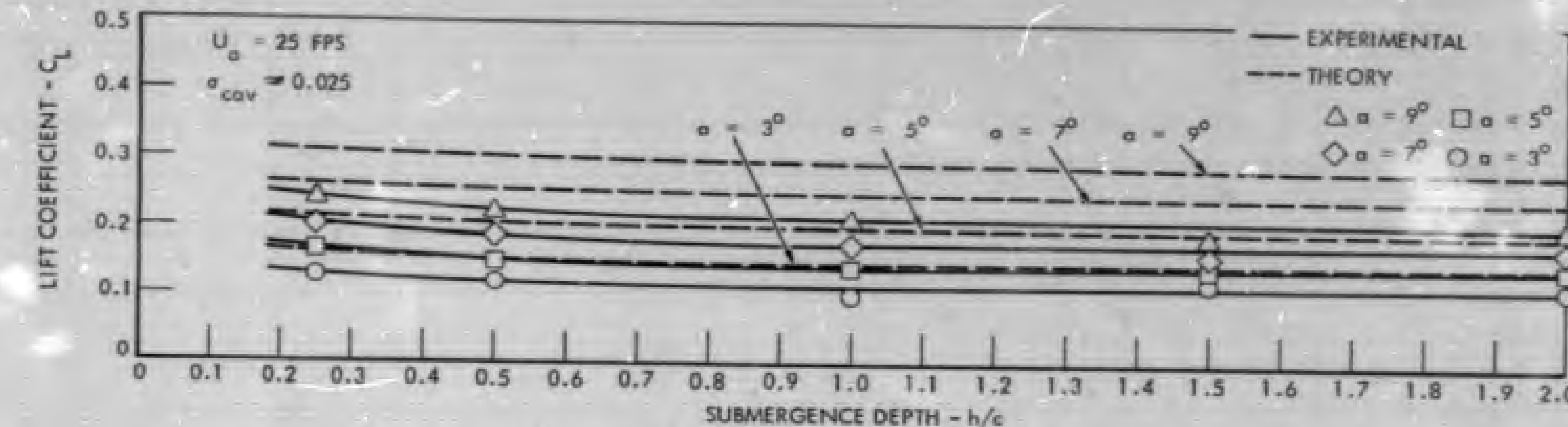

FIGURE 4 - LIFT COEFFICIENT VERSUS SUBMERGENCE DEPTH FOR THICK, CAMBERED SECTION

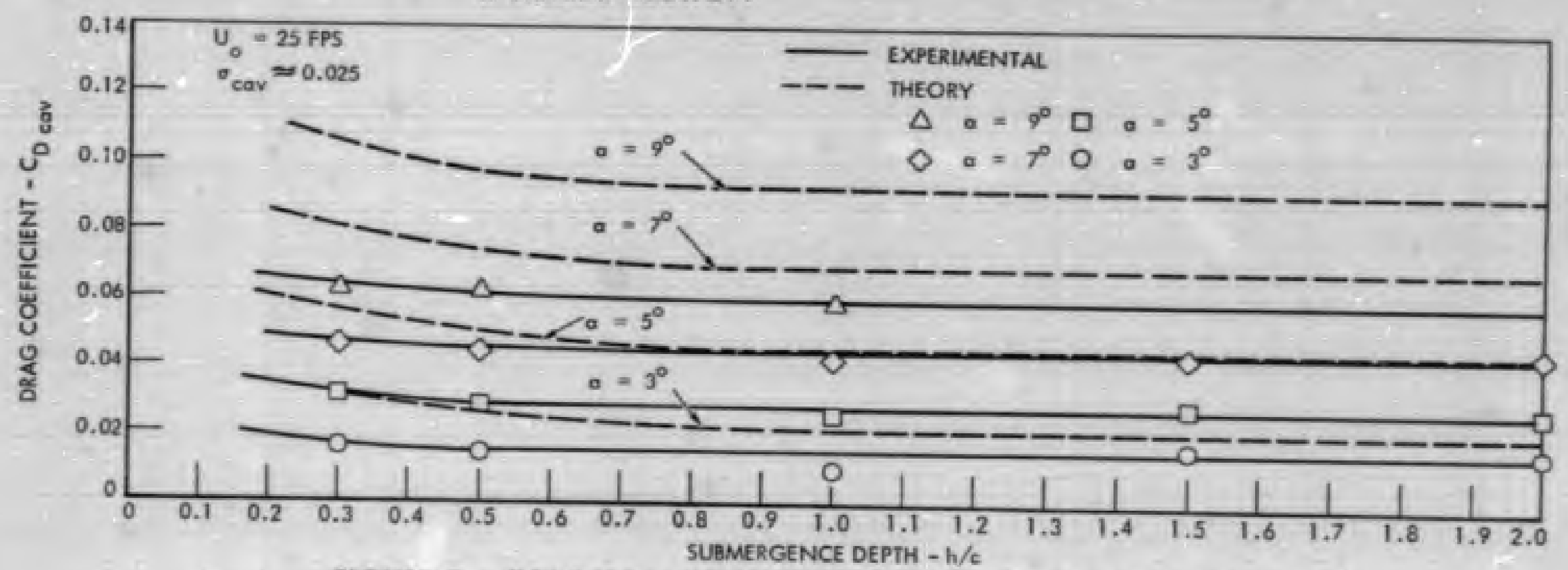

FIGURE 5 - DRAG COEFFICIENT VERSUS SUBMERGENCE DEPTH FOR THICK, CAMBERED SECTION

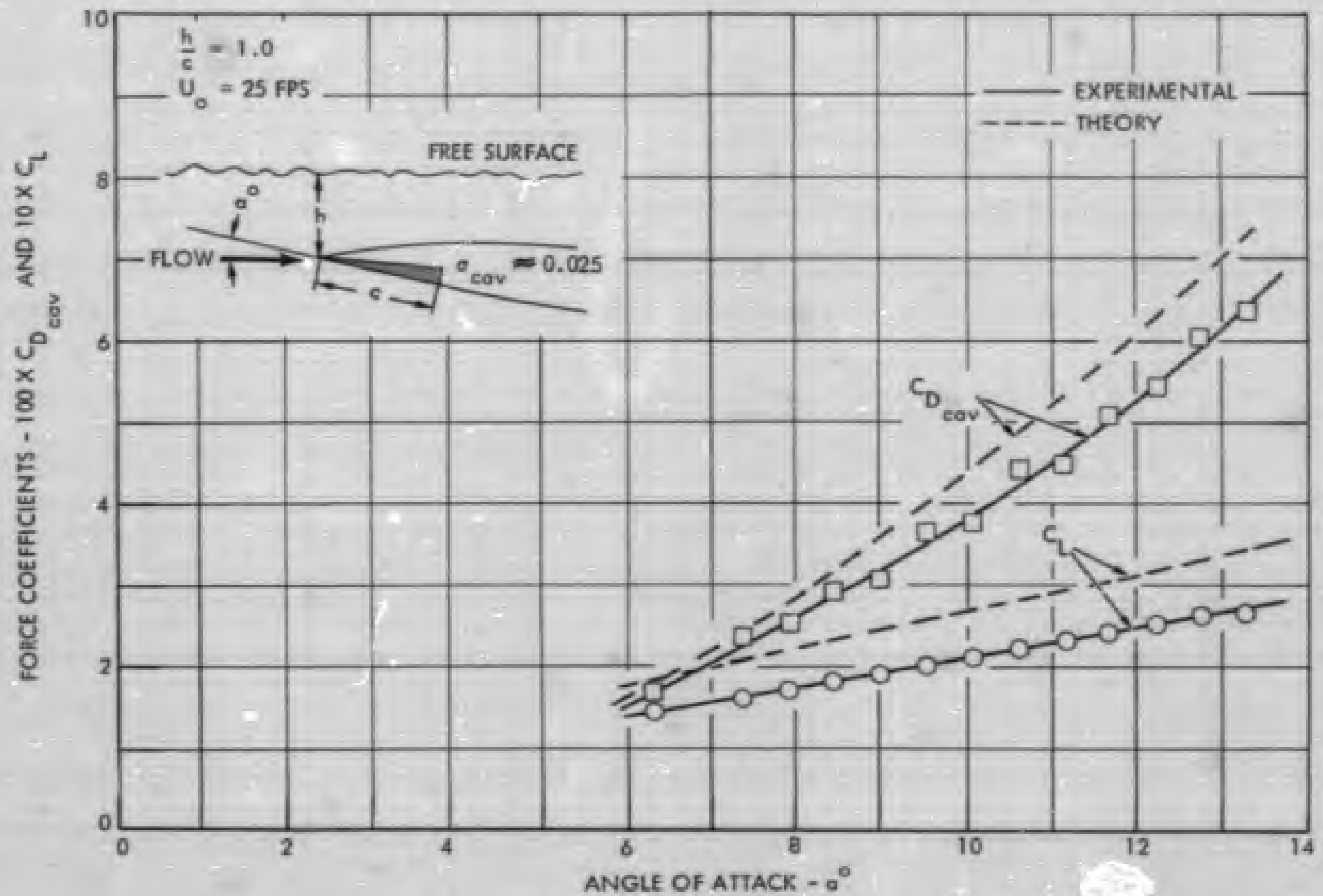

FIGURE 6 - THEORETICAL AND EXPERIMENTAL FORCE COEFFICIENTS FOR WEDGE SECTION

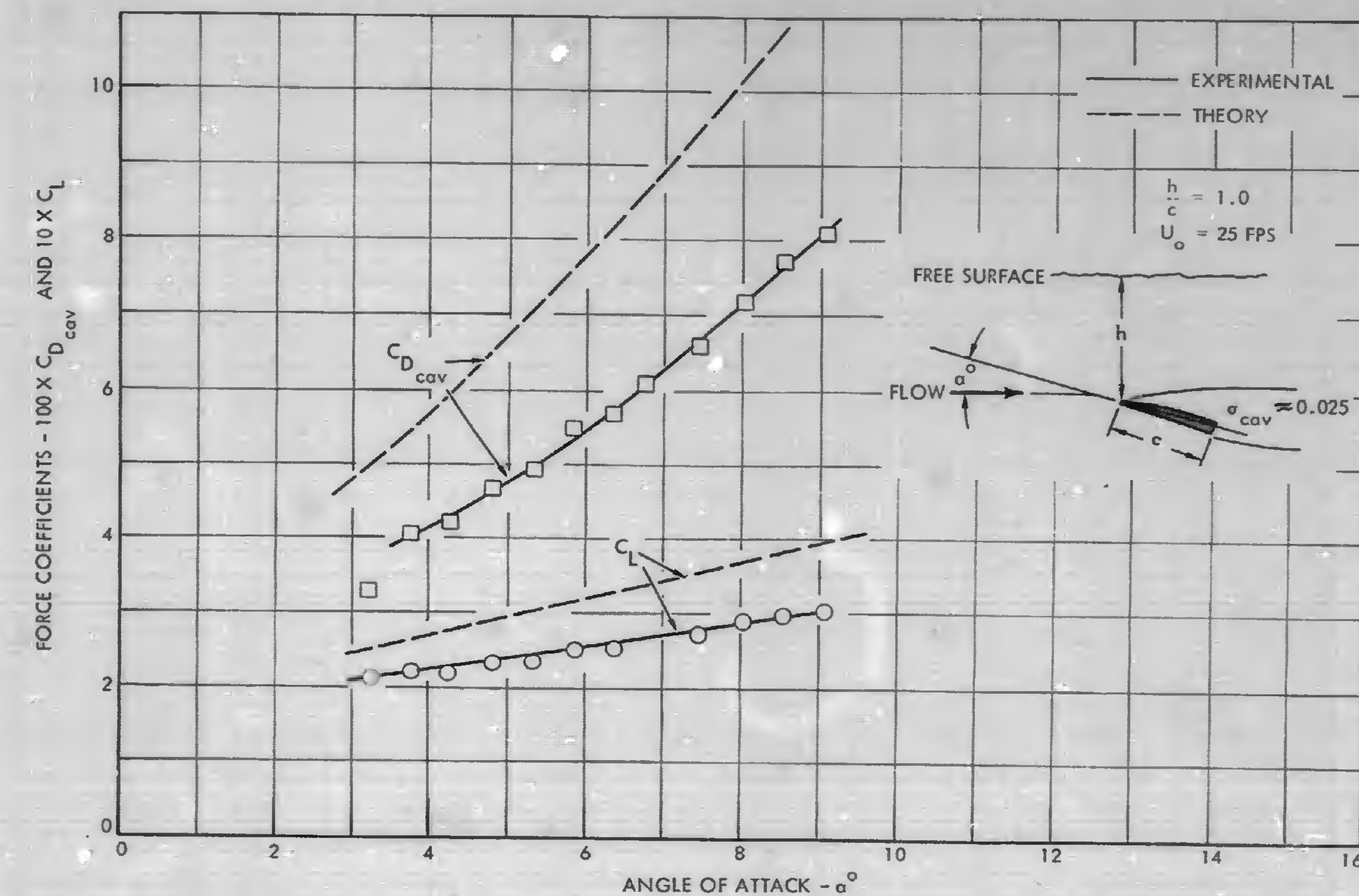

FIGURE 7 - THEORETICAL AND EXPERIMENTAL FORCE COEFFICIENTS FOR THICK, CAMBERED SECTION

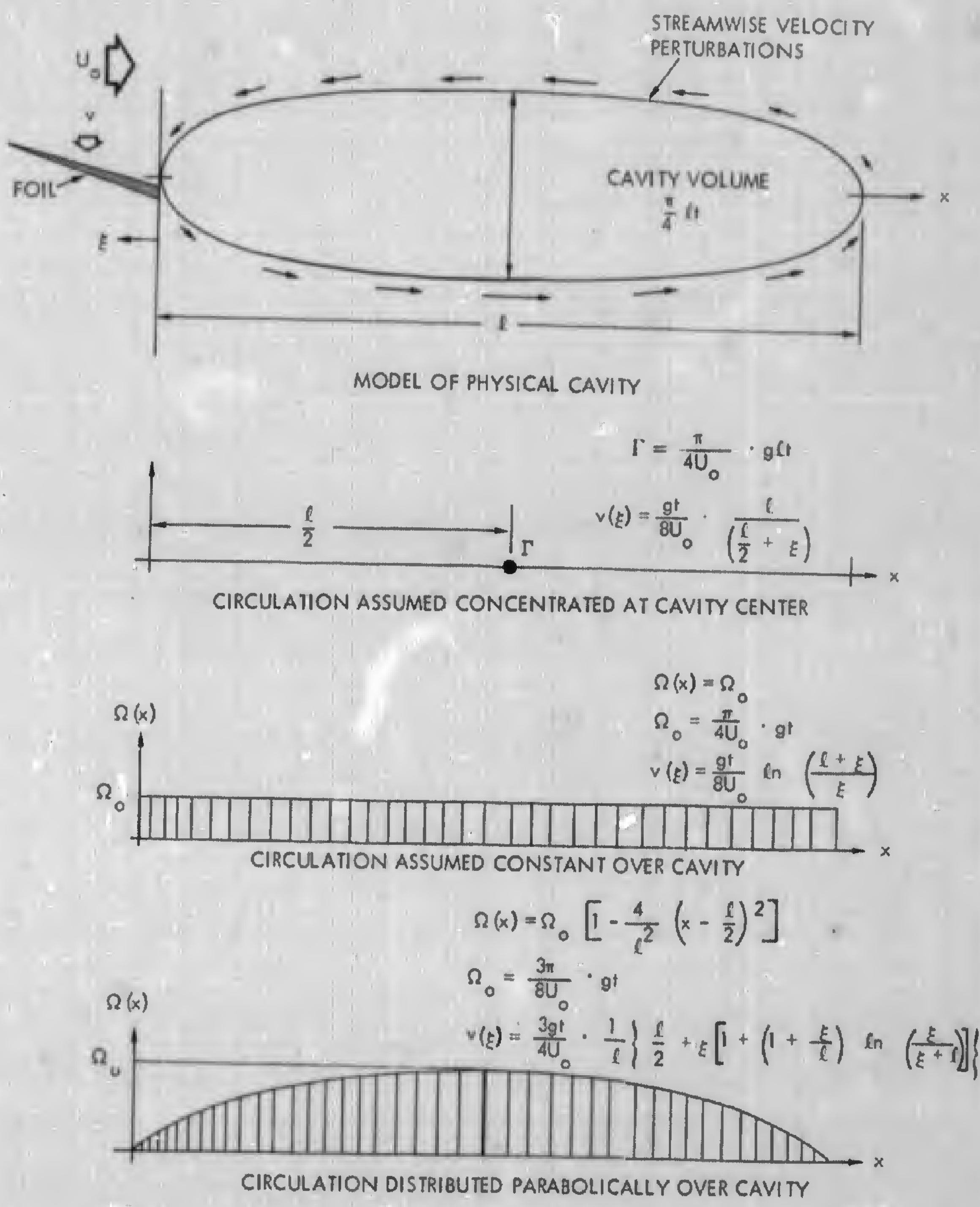

FIGURE 8 - SIMPLE MODELS FOR INDUCED FLOW EFFECTS OF FINITE FROUDE NUMBER OPERATION

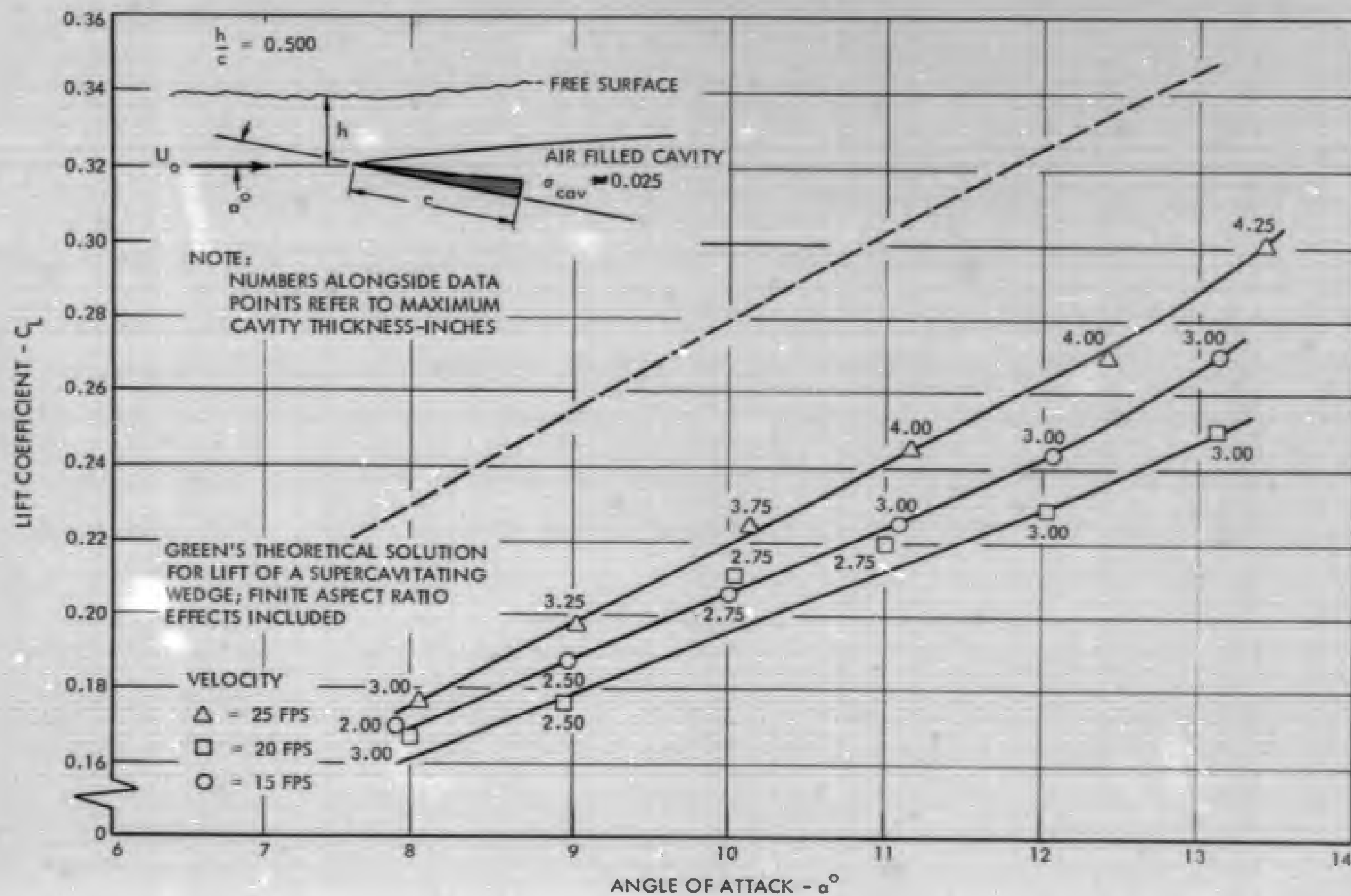

FIGURE 9 - LIFT COEFFICIENT OF WEDGE SECTION AT POSITIVE ANGLES OF ATTACK

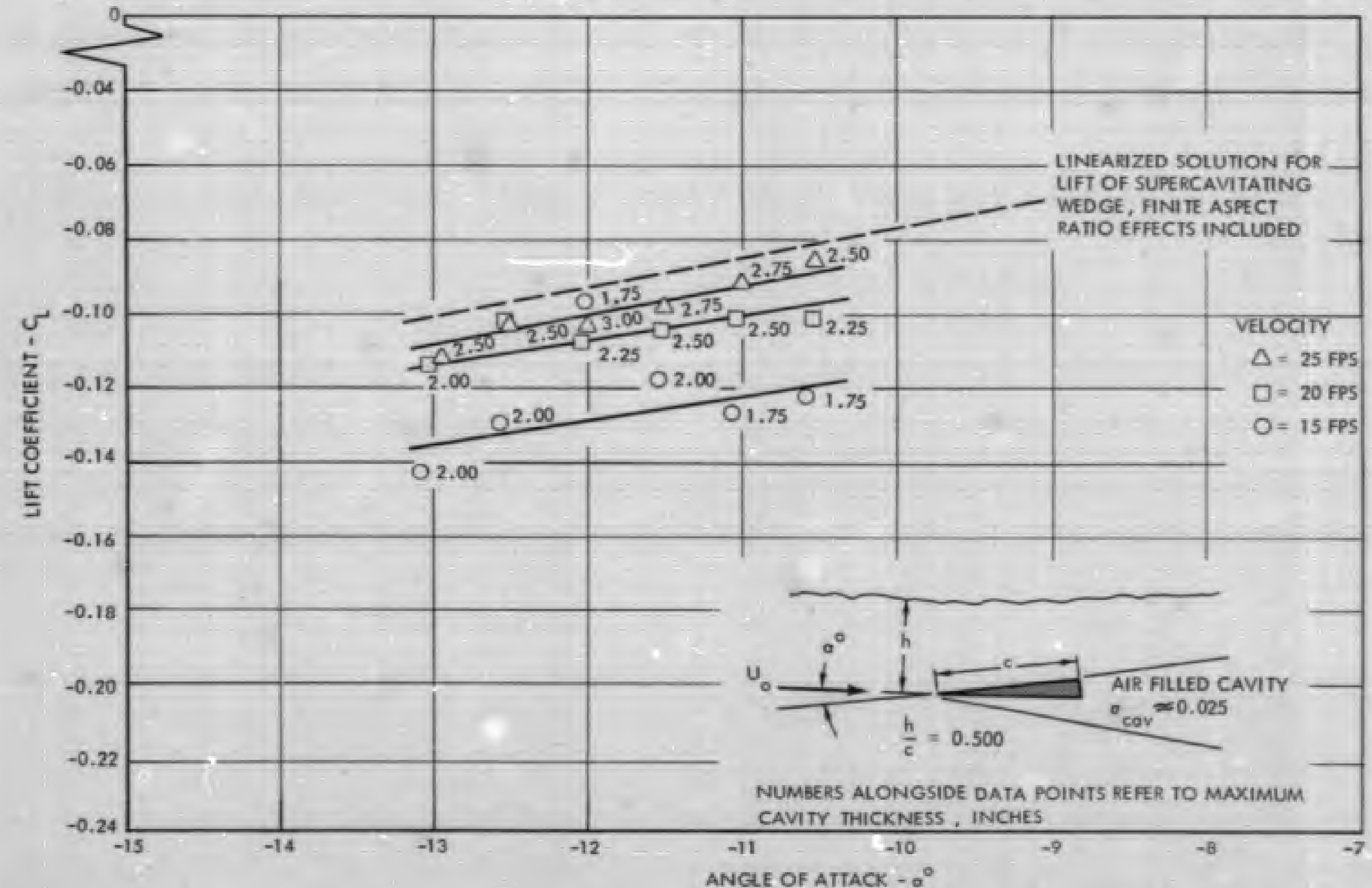

FIGURE 10 - LIFT COEFFICIENT OF WEDGE SECTION AT NEGATIVE ANGLES OF ATTACK

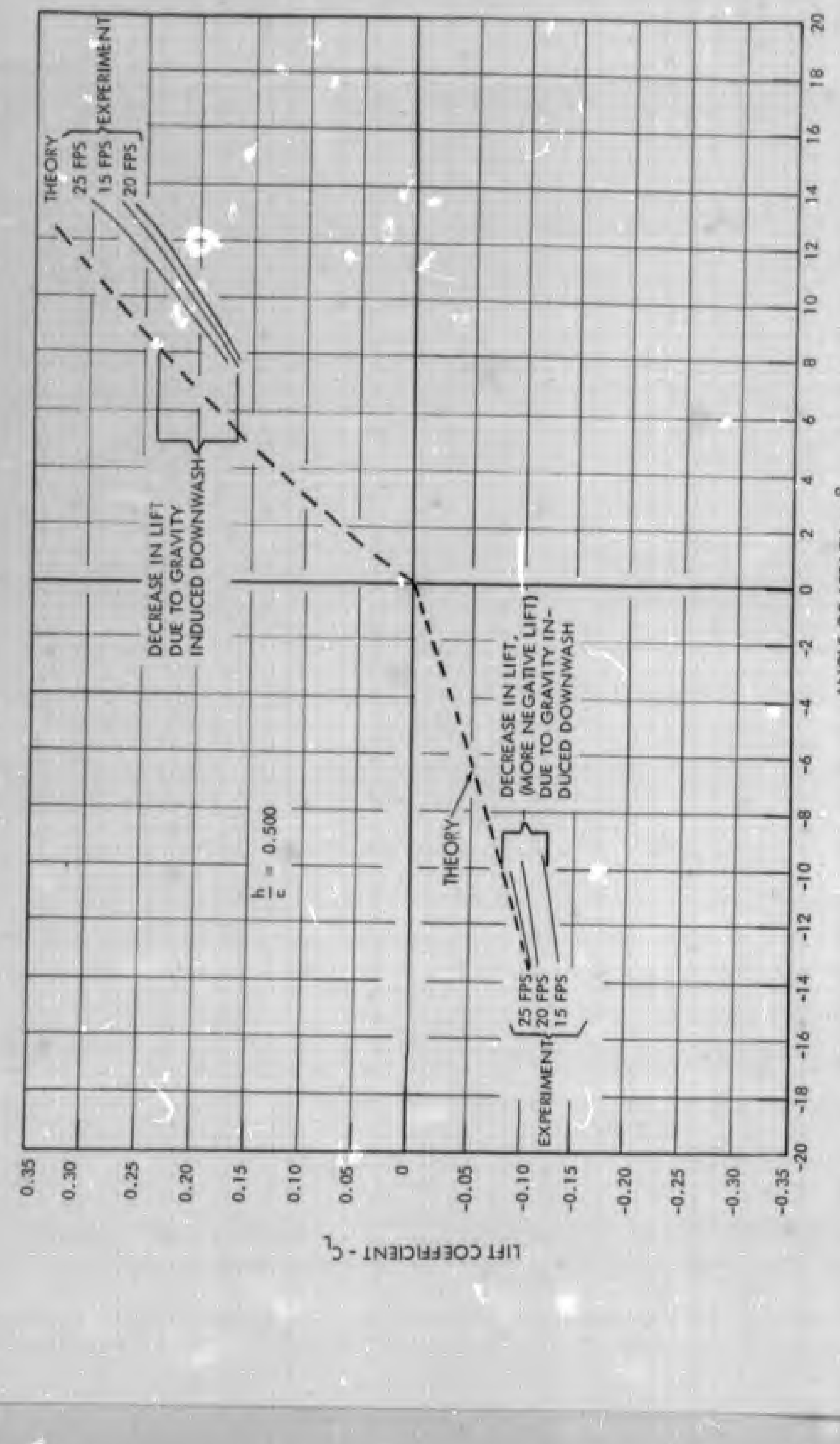

FIGURE 11 - GRAVITY INDUCED DOWNWASH EFFECT ON WEDGE SECTION AT POSITIVE AND NEGATIVE ANGLES OF ATTACK

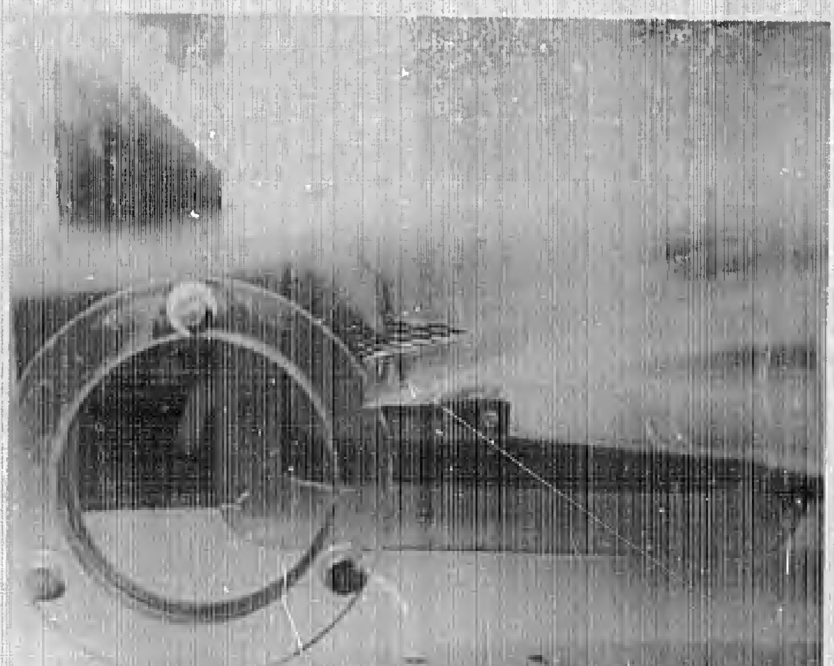

FIGURE 12 - TRACING CAVITY CONTOURS NEAR A DOUBLE-OGIVE STRUT

TABLE OF OFFSETS	
x (INCHES)	y (INCHES)
0.0	0.0
0.145	0.040
0.289	0.057
0.579	0.081
0.869	0.099
1.159	0.114
1.448	0.127
1.737	0.139
2.077	0.151
2.317	0.161
2.607	0.171
2.898	0.180

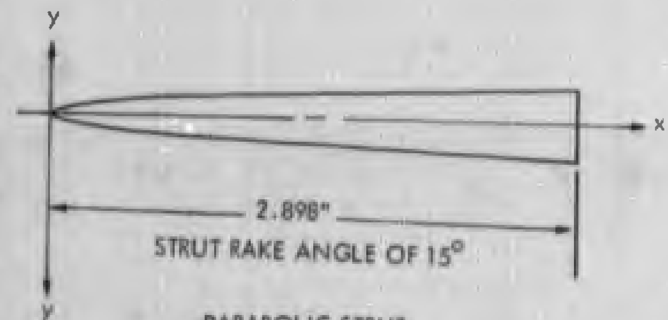

STRUT RAKE ANGLE OF 15°

PARABOLIC STRUT

TABLE OF OFFSETS	
x (INCHES)	y (INCHES)
0.0	0.0
0.289	0.065
0.579	0.115
0.869	0.151
1.159	0.172
1.448	0.179
1.737	0.172
2.077	0.151
2.317	0.115
2.607	0.065
2.898	0.0

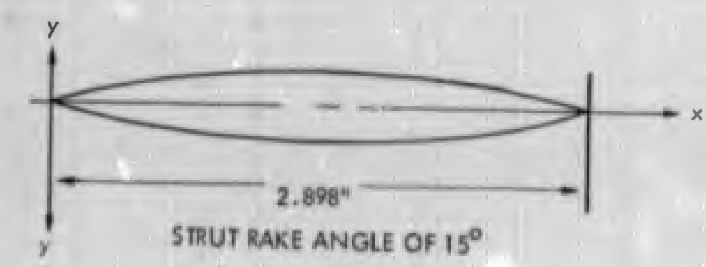

STRUT RAKE ANGLE OF 15°

DOUBLE OGIVE STRUT

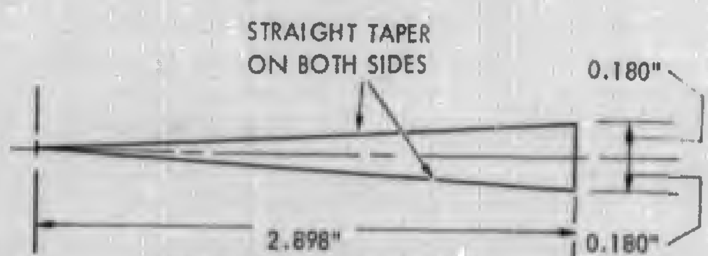

STRUT RAKE ANGLE OF 15°

WEDGE STRUT

FIGURE 13 - OFFSETS OF STRUT SECTIONS TESTED

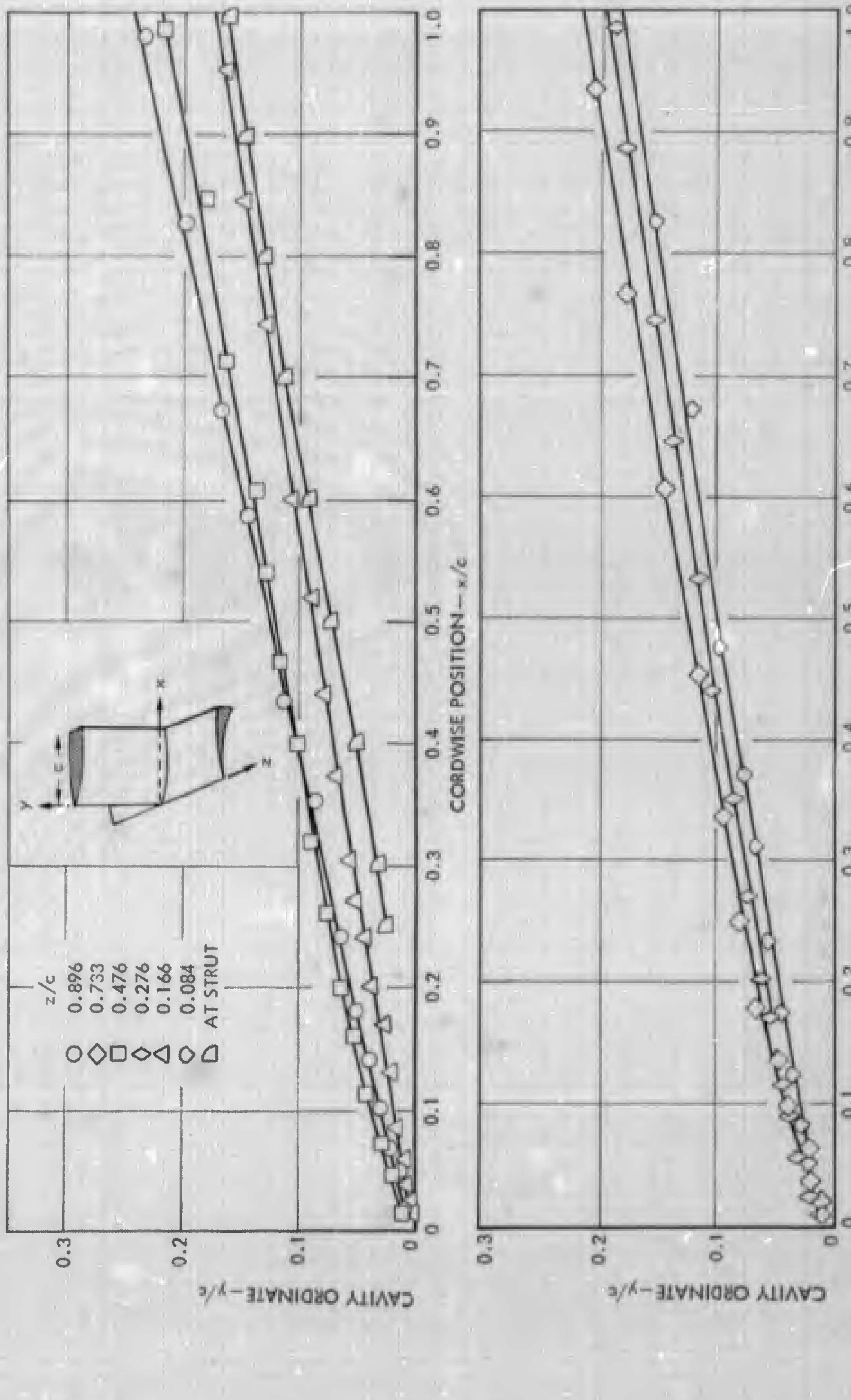

FIGURE 14 - CAVITY CONTOURS NEAR A 12 PERCENT PARABOLIC STRUT

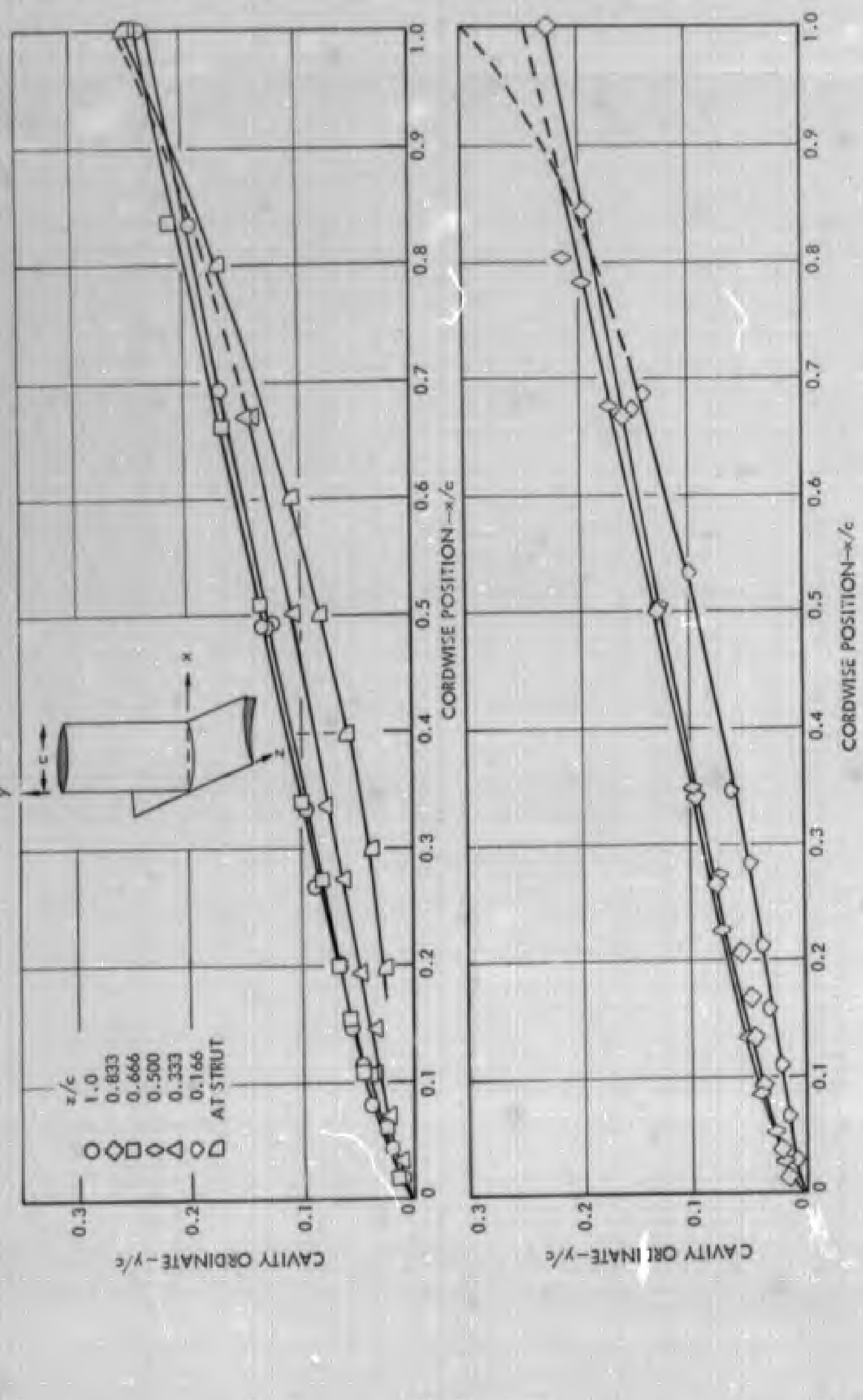

FIGURE 15 - CAVITY CONTOURS NEAR A 12 PERCENT DOUBLE-OGIVE STRUT

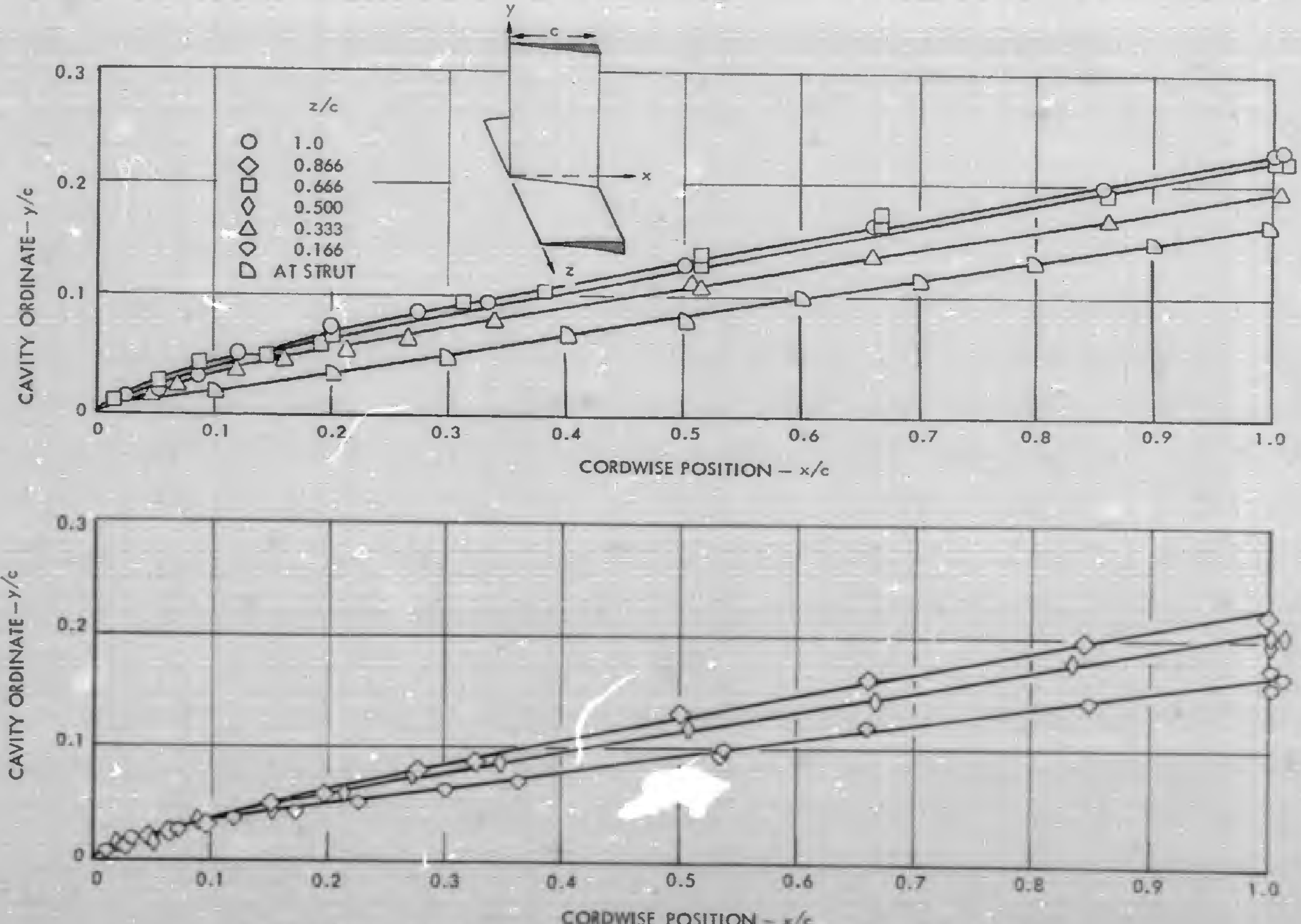

FIGURE 16 - CAVITY CONTOURS NEAR A 12 PERCENT WEDGE STRUT

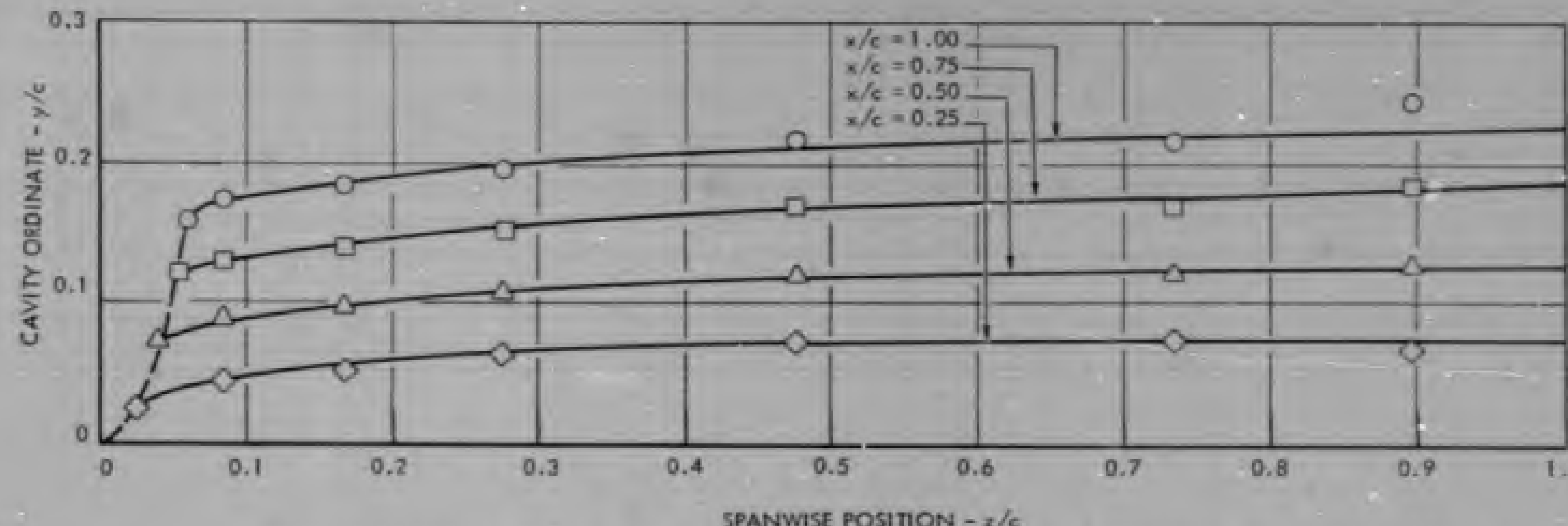

FIGURE 17 (a) - CHANGE IN CAVITY ORDINATE NEAR A12 PERCENT PARABOLIC STRUT

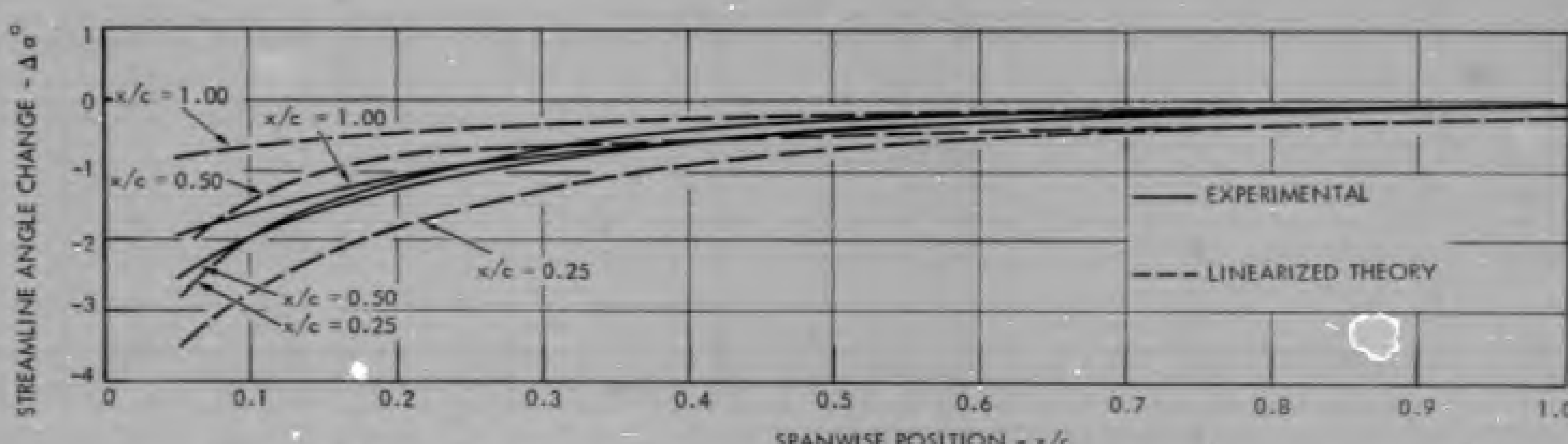

FIGURE 17 (b) - CHANGE IN STREAMLINE ANGLE NEAR A 12 PERCENT PARABOLIC STRUT

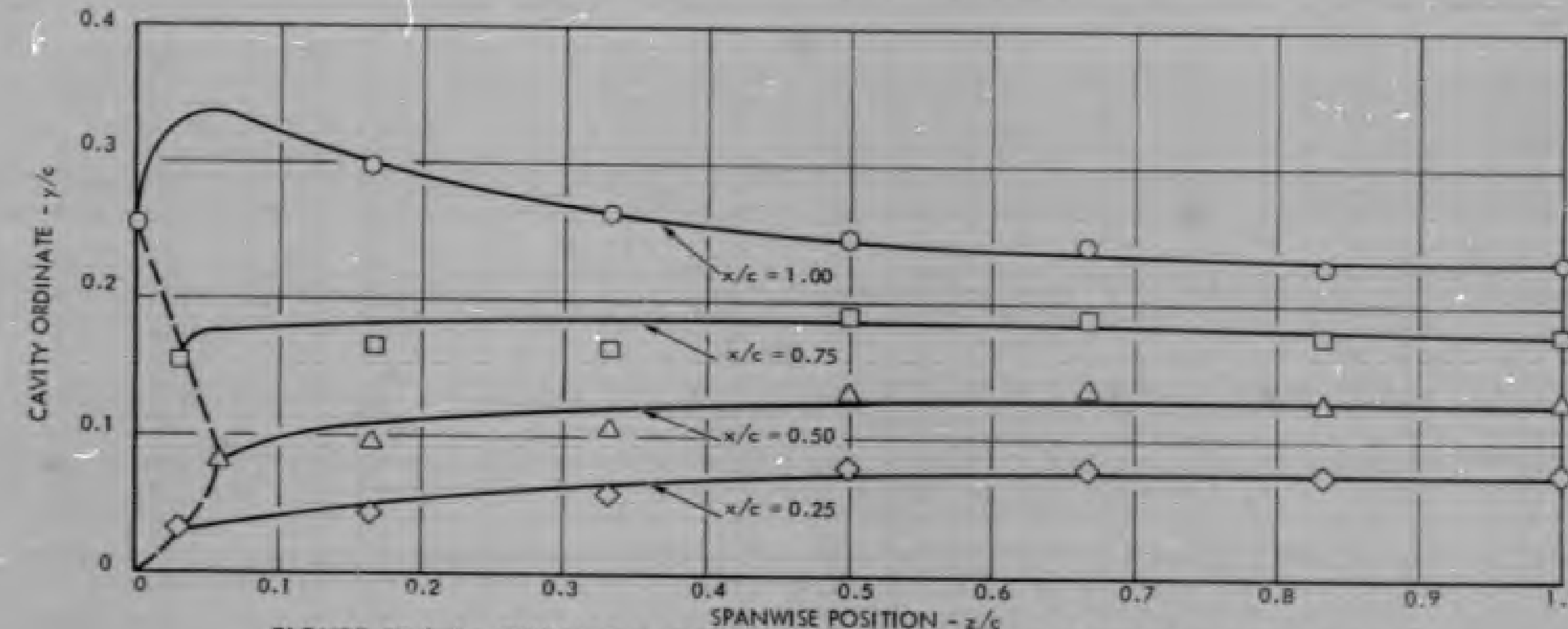

FIGURE 18 (a) - CHANGE IN CAVITY ORDINATE NEAR A 12 PERCENT DOUBLE OGIVE STRUT

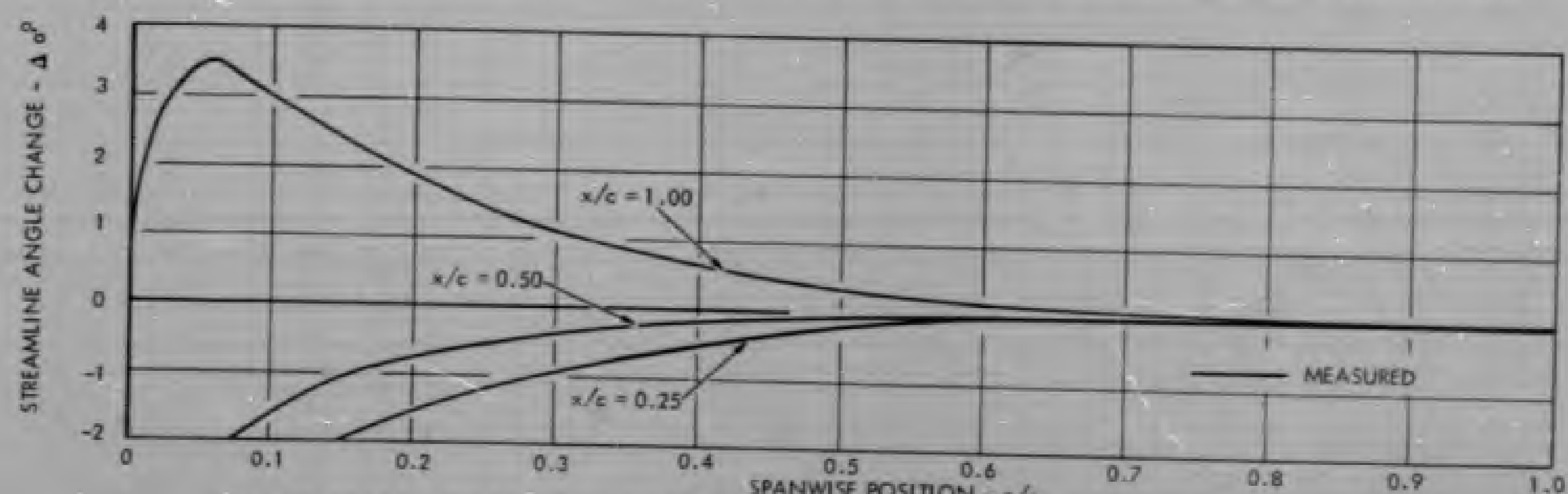

FIGURE 18 (b) - CHANGE IN STREAMLINE ANGLE NEAR A 12 PERCENT DOUBLE OGIVE STRUT

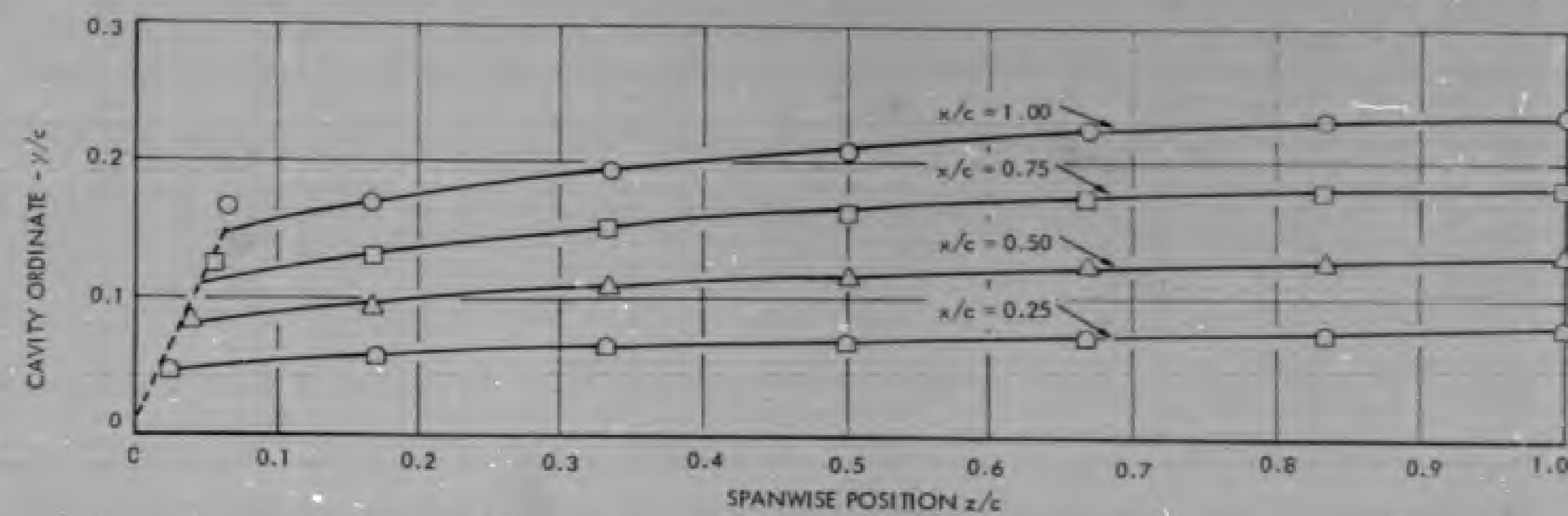

FIGURE 19 (a) - CHANGE IN CAVITY ORDINATE NEAR A12 PERCENT DOUBLE OGIVE STRUT

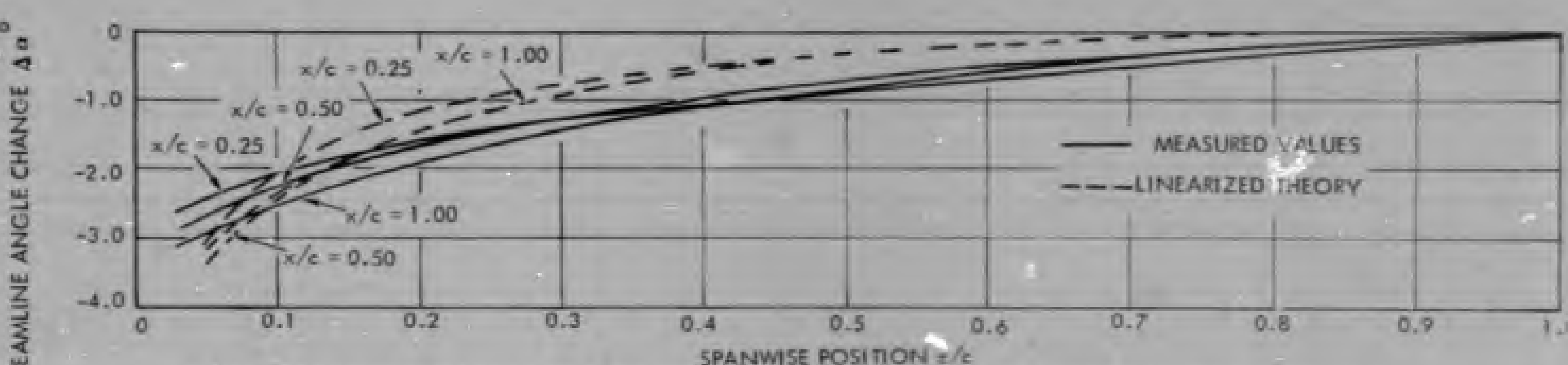

FIGURE 19 (b) - CHANGE IN STREAMLINE ANGLE NEAR A 12 PERCENT WEDGE STRUT

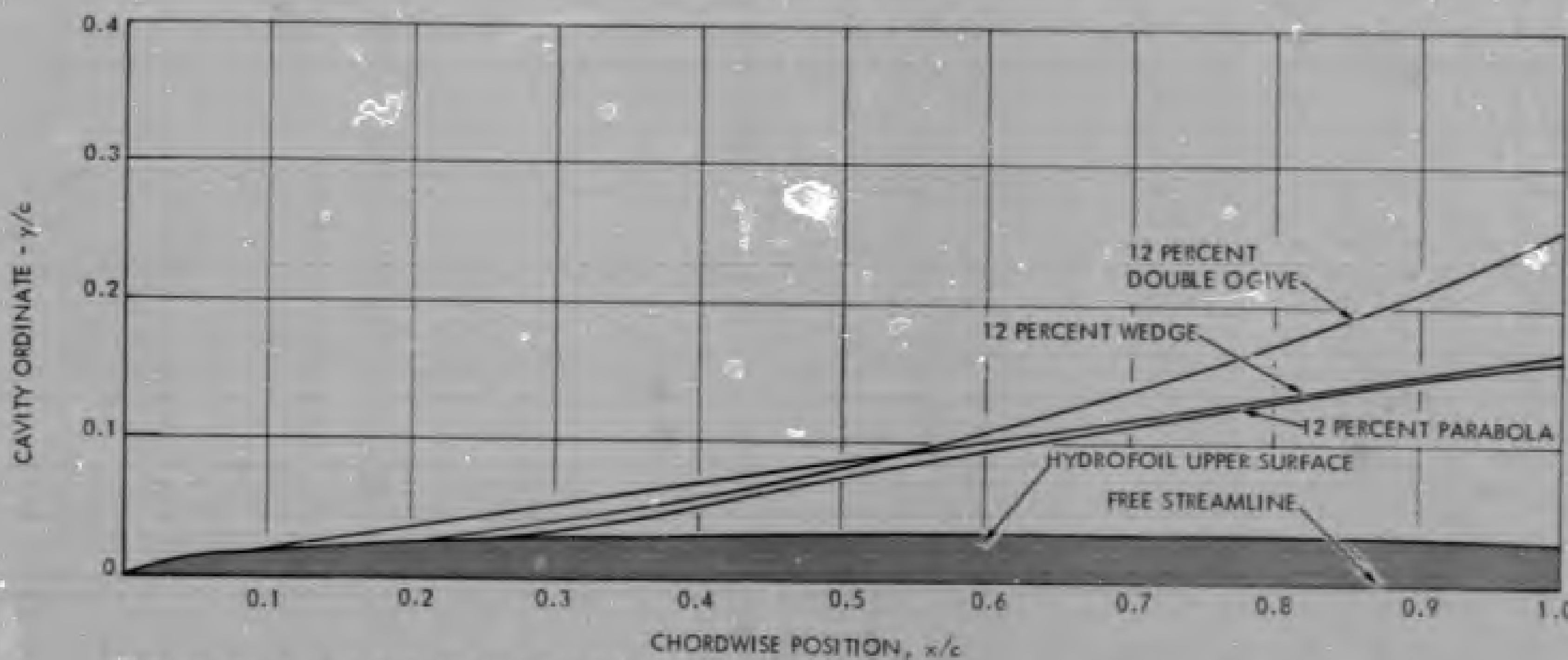

FIGURE 20 - CAVITY ORDINATES AT THE STRUT FOR THREE DIFFERENT STRUT SECTIONS

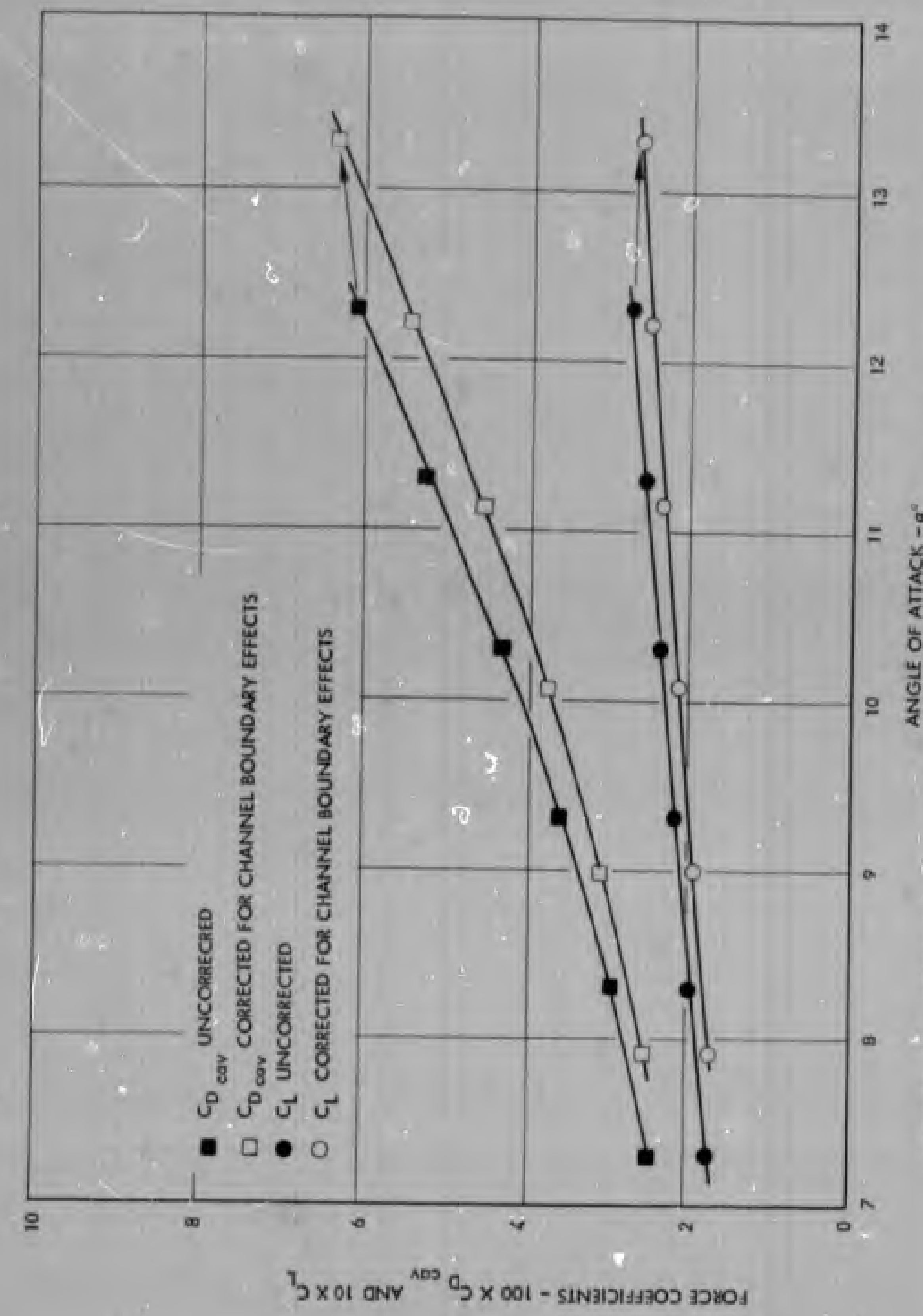

FIGURE 21 - ILLUSTRATING EFFECT OF CHANNEL BOUNDARY CORRECTIONS ON LIFT AND DRAG COEFFICIENTS OF VENTILATED HYDROFOILS

UNCLASSIFIED

Security Classification

DOCUMENT CONTROL DATA - R&D

(Security classification of title, body of abstract and indexing annotation must be entered when the overall report is classified)

1 ORIGINATING ACTIVITY (Corporate author) HYDRONAUTICS, Incorporated Pindell School Road, Howard County, Laurel, Md. 20810	2a REPORT SECURITY CLASSIFICATION Unclassified 2b GROUP

3 REPORT TITLE

EFFECTS OF AMBIENT CONDITIONS, THE GRAVITY FIELD, AND STRUTS, ON FLOWS OVER VENTILATED HYDROFOILS

4 DESCRIPTIVE NOTES (Type of report and inclusive dates)

Technical Report

5 AUTHOR(S) (Last name, first name, initial)

Altmann, R., and Elata, C.

6 REPORT DATE	7a TOTAL NO OF PAGES	7b NO OF REFS
May 1967	61	19

8a CONTRACT OR GRANT NO N00014-66-C0003 b PROJECT NO c d	9a ORIGINATOR'S REPORT NUMBER(S) Technical Report 605-1 9b OTHER REPORT NO(S) (Any other numbers that may be assigned this report)

10 AVAILABILITY/LIMITATION NOTICES

This Document has been approved for Public Release and Sale; Distribution of this document is unlimited.

11 SUPPLEMENTARY NOTES	12 SPONSORING MILITARY ACTIVITY Naval Ship Research and Development Center Department of the Navy

13 ABSTRACT

A series of experiments was conducted to determine the effects on foil performance of changes in cavity pressure and submergence depth. With fully-ventilated foils, drag and lift coefficients were found to be proportional to $(1 + \sigma_{cav})$, as predicted by theory. For base-ventilated foils a different and unexpected dependence of drag and lift on the cavity cavitation number was observed. Lift and drag on fully ventilated hydrofoils were also found to be almost unaffected by changes in submergence depth over the range of practical interest, as predicted by theory. However, the magnitudes of the measured forces were found to be smaller than predicted values. A simple analysis was made of the possible effects of the gravity field on foil performance. Further support for the idea that the gravity field may exert considerable influence was obtained through a series of tests in which ventilated hydrofoils were operated at both positive and negative angles of attack.

Measurements were also made to determine the effects of struts on ventilated hydrofoil cavity contours. Indirectly, these tests also assessed the magnitude of the strut-induced downwash. A considerable downwash was found to exist, having a profound effect on the cavity shape over the hydrofoil. Recent linearized theory on the magnitude of this strut-induced downwash correlates very well with the measurements.

DD FORM 1 JAN 64 1473

023558

UNCLASSIFIED

Security Classification

UNCLASSIFIED

Security Classification

14 KEY WORDS	LINK A		LINK B		LINK C	
	ROLE	WT	ROLE	WT	ROLE	WT
Supercavitating hydrofoils Ventilated cavity flows						

INSTRUCTIONS

1. ORIGINATING ACTIVITY: Enter the name and address of the contractor, subcontractor, grantee, Department of Defense activity or other organization *(corporate author)* issuing the report.

2a. REPORT SECURITY CLASSIFICATION: Enter the overall security classification of the report. Indicate whether "Restricted Data" is included. Marking is to be in accordance with appropriate security regulations.

2b. GROUP: Automatic downgrading is specified in DoD Directive 5200.10 and Armed Forces Industrial Manual. Enter the group number. Also, when applicable, show that optional markings have been used for Group 3 and Group 4 as authorized.

3. REPORT TITLE: Enter the complete report title in all capital letters. Titles in all cases should be unclassified. If a meaningful title cannot be selected without classification, show title classification in all capitals in parenthesis immediately following the title.

4. DESCRIPTIVE NOTES: If appropriate, enter the type of report, e.g., interim, progress, summary, annual, or final. Give the inclusive dates when a specific reporting period is covered.

5. AUTHOR(S): Enter the name(s) of author(s) as shown on or in the report. Enter last name, first name, middle initial. If military, show rank and branch of service. The name of the principal author is an absolute minimum requirement.

6. REPORT DATE: Enter the date of the report as day, month, year; or month, year. If more than one date appears on the report, use date of publication.

7a. TOTAL NUMBER OF PAGES: The total page count should follow normal pagination procedures, i.e., enter the number of pages containing information.

7b. NUMBER OF REFERENCES: Enter the total number of references cited in the report.

8a. CONTRACT OR GRANT NUMBER: If appropriate, enter the applicable number of the contract or grant under which the report was written.

8b, 8c, & 8d. PROJECT NUMBER: Enter the appropriate military department identification, such as project number, subproject number, system numbers, task number, etc.

9a. ORIGINATOR'S REPORT NUMBER(S): Enter the official report number by which the document will be identified and controlled by the originating activity. This number must be unique to this report.

9b. OTHER REPORT NUMBER(S): If the report has been assigned any other report numbers *(either by the originator or by the sponsor)*, also enter this number(s).

10. AVAILABILITY/LIMITATION NOTICES: Enter any limitations on further dissemination of the report, other than those imposed by security classification, using standard statements such as:

(1) "Qualified requesters may obtain copies of this report from DDC."

(2) "Foreign announcement and dissemination of this report by DDC is not authorized."

(3) "U. S. Government agencies may obtain copies of this report directly from DDC. Other qualified DDC users shall request through ________________."

(4) "U. S. military agencies may obtain copies of this report directly from DDC. Other qualified users shall request through ________________."

(5) "All distribution of this report is controlled. Qualified DDC users shall request through ________________."

If the report has been furnished to the Office of Technical Services, Department of Commerce, for sale to the public, indicate this fact and enter the price, if known.

11. SUPPLEMENTARY NOTES: Use for additional explanatory notes.

12. SPONSORING MILITARY ACTIVITY: Enter the name of the departmental project office or laboratory sponsoring *(paying for)* the research and development. Include address.

13. ABSTRACT: Enter an abstract giving a brief and factual summary of the document indicative of the report, even though it may also appear elsewhere in the body of the technical report. If additional space is required, a continuation sheet shall be attached.

It is highly desirable that the abstract of classified reports be unclassified. Each paragraph of the abstract shall end with an indication of the military security classification of the information in the paragraph, represented as *(TS)*, *(S)*, *(C)*, or *(U)*.

There is no limitation on the length of the abstract. However, the suggested length is from 150 to 225 words.

14. KEY WORDS: Key words are technically meaningful terms or short phrases that characterize a report and may be used as index entries for cataloging the report. Key words must be selected so that no security classification is required. Identifiers, such as equipment model designation, trade name, military project code name, geographic location, may be used as key words but will be followed by an indication of technical context. The assignment of links, roles, and weights is optional.

DD FORM 1 JAN 64 1473 (BACK)

UNCLASSIFIED

Security Classification